

# 1. KdV-Class Solitons

## 1.1 Korteweg–de Vries Equation and KdV-Class Equations

In this section, we derive the KdV equation from the full set of hydrodynamic equations. Here, we realize the general approach, i.e., we do not consider any particular type of a medium (Sect. 1.1.1), and work further with the general equations. We demonstrate that the KdV model is universal in the sense that it describes the nonlinear wave dynamics in any medium where the wave dispersion is of a certain class, and consider the scale transformations and the similarity principle for the KdV equation (Sect. 1.1.2). We also briefly consider some other one-dimensional equations of the KdV class.

### 1.1.1 Derivation of the KdV Equation

The fundamental equation describing the propagation of nonlinear waves in the one-dimensional case in a medium with weak dispersion is the *Korteweg–de Vries equation* (*KdV equation*) [12], with solutions as stable solitary wave structures, i.e., *solitons*. Let us show how this equation can be derived.

Introduce, first of all, the generalized “density”  $\rho$  and generalized “sound” velocity  $c(\rho)$ , neglecting the medium’s dispersion for the moment.

- For the *surface waves* in the water the above are:  $\rho = H$  is the depth and  $c(\rho)$  is the phase velocity of the waves;  $c(\rho) = c_0 = \sqrt{gH}$  for small-amplitude waves.
- For the *ion-acoustic waves* in a collisionless plasma:  $\rho$  is the plasma (gas) density and  $c(\rho)$  is the phase velocity of the ion sound;  $c(\rho) = c_s = \sqrt{T_e/m_i}$  for the long-wavelength linear waves, where  $T_e$  is the electron temperature in energy units (Boltzmann constant equals unity), and  $m_i$  is the ion mass.
- For the *magnetosonic waves* in a magnetized plasma:  $\rho = |\mathbf{B}_0|$  is (the strength of) the external magnetic field and  $c(\rho) = v_A = |\mathbf{B}_0|/\sqrt{4\pi nm}$  is the Alfvén velocity, in this case usually the plasma density  $nm \approx n_i m_i$  where  $n_i$  is the ion density.

In the following, we work with equations involving these generalized functions. We assume the dissipation is negligible and choose the following as the basic the set of gas dynamics (or hydrodynamics) equations:

$$\begin{aligned}\partial_t \mathbf{v} + (\mathbf{v} \cdot \nabla) \mathbf{v} + (c^2/\rho) \nabla \rho &= 0, \\ \partial_t \rho + \nabla \cdot (\rho \mathbf{v}) &= 0.\end{aligned}\tag{1.1}$$

These are the equation of motion and the continuity equation for the generalized velocity and density, respectively. For the *surface waves* in shallow water,  $\mathbf{v}$  is the hydrodynamic velocity in the wave (the “mass” velocity); for the *ion-acoustic waves* it is the ion velocity, for the *magnetosonic waves*  $\mathbf{v} = \mathbf{h} \equiv \mathbf{B}_\sim/|\mathbf{B}_0|$  is the wave magnetic field normalized to the external magnetic field.

Assuming that the gas motion is a potential one, i.e.,  $\mathbf{v} = \nabla \Phi$ , we integrate the first equation of the set (1.1) and obtain

$$\partial_t \Phi + \frac{1}{2} (\nabla \Phi)^2 + \frac{c^2(\rho - \rho_0)}{2\rho} + \frac{c^2 z}{\rho} = 0,\tag{1.2}$$

where  $\rho_0 = \text{const.}$  The continuity equation for the velocity,  $\nabla \cdot \mathbf{v} = 0$ , gives the Laplace equation

$$\Delta \Phi = 0.\tag{1.3}$$

We supplement this set by the boundary conditions

$$\begin{aligned}\partial_t \eta + \partial_x \eta \partial_x \Phi + \partial_y \eta \partial_y \Phi - \partial_z \Phi &= 0, \\ \partial_t \Phi + (\nabla \Phi)^2/2 + (c^2/\rho) \eta &= 0, \\ z = \eta(x, y, t), \\ \partial_z \Phi|_{z=-\rho_0} &= 0,\end{aligned}\tag{1.4}$$

where for a fluid, for example, the third and fourth conditions can be interpreted as the equation of the fluid surface and the boundary condition on the bottom, i.e., at  $z = -H$ .

We have now the full set of equations. We then introduce small parameters  $\mu = v_0/c \ll 1$  and  $\varepsilon = \rho_0/l \ll 1$  (here,  $l$  is the characteristic linear scale of perturbations and  $v_0$  is the amplitude of the particle velocity in the wave, note also that  $\varepsilon^2 \sim \mu$ ), expand the equations into the series of  $\mu$  and  $\varepsilon$ , and convert the obtained expressions to dimensionless variables:

$$\begin{aligned}x' &= x/l, \quad y' = y/l, \quad z' = z/\rho_0, \quad t' = c_0 t/l, \\ \Phi' &= \Phi/v_0 l, \quad \eta' = c_0 \eta/v_0 \rho_0, \quad c_0 = \sqrt{g \rho_0}.\end{aligned}$$

In the linear approximation in  $\mu$  and  $\varepsilon^2$  we obtain

$$\begin{aligned}\partial_{z'}^2 \Phi' + \varepsilon^2 (\partial_{x'}^2 \Phi' + \partial_{y'}^2 \Phi') &= 0, \\ \partial_{t'} \Phi' + \frac{\mu}{2} [(\partial_{x'} \Phi')^2 + (\partial_{y'} \Phi')^2] + \frac{\mu}{2\varepsilon^2} (\partial_{z'} \Phi')^2 + \eta'|_{z'=\mu\eta'} &= 0, \\ \Phi'|_{z'=-1} &= 0.\end{aligned}\tag{1.5}$$

The first of these equations is obtained from the Laplace equation (1.3), the second from the equation of motion for the potential  $\Phi$ , and the third from

the last boundary condition of set (1.4). Expanding the potential  $\Phi$  in  $z'$ , we obtain from Eqs. (1.5)

$$\partial_{t'}\varphi' + \frac{\mu}{2}(\nabla\varphi')^2 + \eta' = O(\varepsilon^4, \mu^2, \varepsilon^2\mu)$$

and

$$\partial_{t'}\eta' + \mu\nabla\varphi' \cdot \nabla\eta' + \mu\eta'\Delta\varphi' + \Delta\varphi' + \frac{\varepsilon^2}{3}\Delta^2\varphi' = O(\varepsilon^4, \mu^2, \varepsilon^2\mu),$$

where  $\varphi' = \Phi'|_{z'=0}$ . Now return back to the old variables, introduce the new potential  $\psi = \varphi + \rho_0^2\Delta\varphi/3$ , where  $\varphi = v_0 l\varphi' - c_0 t$ , and write with the accepted accuracy

$$\begin{aligned} \partial_t\psi + (\nabla\psi)^2/2 + c^2 + 2c_0\beta\Delta\rho/\rho_0 &= 0, \\ \partial_t\rho + \nabla \cdot (\rho\nabla\psi) &= 0, \end{aligned} \tag{1.6}$$

where  $\beta = c_0\rho_0^2/6$  and  $\rho = \rho_0 + \eta(t, x, y)$ . Eqs. (1.6) are the equation of motion for the potential  $\psi$  and the continuity equation for the generalized density  $\rho$ . Here,  $\beta$  is the dispersion parameter, and the last equation, for example, for waves on the fluid surface can be interpreted in the following way: the height of the fluid level is a sum of the depth of the “tank” (where the fluid is contained) and the height of the perturbation set by the equation of the surface.

Now, if instead of the potential  $\psi$  we introduce the velocity

$$\mathbf{v}(t, x, y) = \nabla\psi(t, x, y)$$

and apply the gradient to the first equation of (1.6), we obtain

$$\begin{aligned} \partial_t\mathbf{v} + (\mathbf{v}\nabla)\mathbf{v} + c^2\nabla\rho/\rho_0 + 2c_0\beta\nabla\Delta\rho/\rho_0 &= 0, \\ \partial_t\rho + \nabla(\rho\mathbf{v}) &= 0. \end{aligned} \tag{1.7}$$

Set (1.7) represents the *Boussinesq equations* describing waves on the surface of shallow water as well as waves in plasmas and other dispersive media. These are three-dimensional nonlinear evolution equations, and it is generally very difficult to solve them.

Assume that  $v_0/c$ ,  $(\rho - \rho_0)/\rho_0$ , and  $\delta/\lambda$  are small (of the first order in  $\mu$ ),  $\varepsilon^2$  (here,  $\delta = (|\beta|/c_0)^{1/2}$  is the effective dispersion length, and  $\lambda$  is the characteristic wavelength). Further we suppose (as in standard hydrodynamics) that

$$c^2(\rho) = c_0^2(\rho/\rho_0)^{\gamma-1}, \quad \text{and} \quad \gamma = c_p/c_v,$$

and look for a solution of (1.7) written as

$$\rho(t, x) = \rho(v) + \varphi(t, x), \tag{1.8}$$

where

$$\begin{aligned}\rho(v) &= \pm c(v) d_v \rho, \\ c(v) &= c_0 + (\gamma - 1)v/2,\end{aligned}\tag{1.9}$$

and  $\varphi(t, x)$  is small (of the second order in  $\mu, \varepsilon^2$ ). Then consider a wave propagating in the positive direction of the  $x$ -axis. Neglecting the terms of order higher than the second, we find that the function  $\varphi(t, x)$  satisfies the equation

$$\partial_t \varphi + c_0 \partial_x \varphi = 0.$$

Substituting (1.8) into (1.7), using expressions (1.9), and excluding the potential  $\varphi$  from the obtained expressions, we have

$$\partial_t v + \left( c_0 + \frac{\gamma + 1}{2} v \right) \partial_x v + \beta \partial_x^3 v = 0.\tag{1.10}$$

Converting now to new variables

$$\xi = x - c_0 t \quad \text{and} \quad u = \frac{\gamma + 1}{2} v,$$

we finally obtain from (1.10)

$$\partial_t u + u \partial_\xi u + \beta \partial_\xi^3 u = 0.\tag{1.11}$$

This is the *Korteweg-de Vries equation* (*KdV equation*) written in the reference frame moving with the velocity  $c_0$  along the  $x$ -axis. It is obvious that this equation is much simpler than the initial three-dimensional set of hydrodynamic equations or Boussinesq equations.

We thus realized the marvelous ideas of Korteweg and de Vries that: to investigate complex nonlinear equation(s), we can simplify them while preserving their basic qualitative features; it is necessary, with the same order of accuracy, to keep the terms leading to the opposite effects, in our case - to maintain the balance of the nonlinear and dispersive terms.

It is very important that the KdV equation has an infinite number of the integrals of motion; this determines its complete integrability. Consider briefly this problem and rewrite the *KdV equation* (1.11) as

$$\partial_t u + \partial_x (u^2/2 + \beta \partial_x^2 u) = 0.\tag{1.12}$$

Equation (1.12) has the form of the conservation law for the “momentum” of the system,

$$\mathcal{J}_1 = \int_{-\infty}^{\infty} u(t, x) dx = \text{const}.\tag{1.13}$$

Analogously we can obtain the next integrals of motion for the higher orders of  $u$  [3]:

$$\partial_t (u^2/2) + \partial_x \{ u^3/3 + \beta [u \partial_x^2 u - (\partial_x u)^2] \} = 0\tag{1.14}$$

and

$$\partial_t(u^3/3 - \beta\partial_x^2 u) + \partial_x \{u^4/4 + \beta[u^2\partial_x^2 u + 2\partial_t u\partial_x u] + \beta^2(\partial_x^2 u)^2\} = 0. \quad (1.15)$$

Equation (1.14) can be interpreted as the conservation law for the “energy” of the system [3], and equation (1.15), first obtained by Whitham [88], does not have any obvious physical interpretation. Other conservation laws were obtained by Kruskal, Zabusky and Miura [89] who also proved [90,91] that the KdV equation has an infinite number of conserved integrals, i.e., invariants given by

$$\mathcal{I}_m = \int_{-\infty}^{\infty} Q_m(t, x) dx. \quad (1.16)$$

For example, the first six invariants are [89–91]<sup>1</sup>

$$\begin{aligned} Q_1 &= u, & Q_2 &= u^2/2, & Q_3 &= u^3/3 - \beta(\partial_x u)^2, \\ Q_4 &= u^4/4 - 3\beta u(\partial_x u)^2 + 2\beta^2(\partial_x^2 u)^2/5, \\ Q_5 &= u^5/5 - 6\beta u^2(\partial_x u)^2 + 36\beta^2 u(\partial_x^2 u)^2/5 - 108\beta^3(\partial_x^3 u)^2/35, \end{aligned}$$

and

$$\begin{aligned} Q_6 &= u^6/6 - 10\beta u^3(\partial_x u)^2 + \beta^2[-5(\partial_x u)^4 + 18u^2(\partial_x^2 u)^2] \\ &\quad + \beta^3[-108u(\partial_x^3 u)^2/7 + 120(\partial_x^2 u)^3/7] + 36\beta^4\partial_x^4 u. \end{aligned}$$

As we already noted, the infinite number of the *conservation laws* proves that the KdV equation represents a completely integrable system; we will also see that in the next section.

### 1.1.2 Universality of the KdV Model. Scaling Transformations and Similarity Principle

It is important that the KdV equation is universal in the sense that it describes the propagation of nonlinear waves when the linearized wave dispersion law is given by

$$\omega = c_0 k \left(1 - \frac{\beta k^2}{c_0}\right). \quad (1.17)$$

For example, this is the case for:

(a) *Surface waves* in shallow water where  $u$  is the amplitude of the hydrodynamic velocity (in some sense – the amplitude of the wave),  $\beta = c_0(H^2 - 3\sigma/\rho g)/6$  for the gravity-capillary waves, and  $\beta = c_0 H^2/6$  for the gravity waves.

---

<sup>1</sup> Detailed information on this problem including a general algorithm to calculate the numerical factors in  $Q_m$  can be found in Refs. [90,92].

(b) *Ion-acoustic waves* in an unmagnetized plasma where  $u$  is the velocity of the ion sound wave,  $\beta = c_s r_D^2/2$ ,  $r_D = (T_e/4\pi n_e e^2)^{1/2}$  is the electron Debye length, and  $n_e$  is the unperturbed number density of plasma electrons.

(c) *Magnetosonic waves* in a magnetized plasma where  $u$  is the normalized wave magnetic field perturbation,

$$\beta = v_A \frac{c^2}{2\omega_{pi}^2} \left( \frac{m_e}{m_i} - \cot^2 \theta \right),$$

$c$  is the speed of light,  $\omega_{pi} = (4\pi n_i e^2/m_i)^{1/2}$  is the ion plasma frequency,  $m_e$  is the electron mass, and  $\theta$  is the angle between the direction of the wave propagation (vector  $\mathbf{k}$ ) and the external magnetic field  $\mathbf{B}_0$ .<sup>2</sup>

The *KdV equation* is often written in a slightly different form, e.g.,

$$\partial_t u + \alpha u \partial_x u + \beta \partial_x^3 u = 0, \quad (1.18)$$

which can be easily obtained from (1.11) via the scale transformations  $u \rightarrow \alpha u$ ,  $t \rightarrow t$ , and  $\xi \rightarrow x$ . For the analytical (exact) integration using the *inverse scattering transform* method (*IST method*) (see Sect. 1.2) the KdV equation (1.11) is transformed by  $u \rightarrow -6u$ ,  $t \rightarrow t$ , and  $\xi \rightarrow x$ . In this case, the equation for  $\beta = 1$  is given by

$$\partial_t u - 6u \partial_x u + \partial_x^3 u = 0. \quad (1.19)$$

The negative sign of the dispersion term can be obtained by the change  $u \rightarrow -u$  and  $x \rightarrow -x$ . The sign of  $\alpha$  in (1.18) determines the “polarity” of the solution (which can be positive,  $u > 0$ , or negative,  $u < 0$ ), while the sign of  $\beta$  determines the direction of the wave propagation. Thus the KdV equation can be equally applied to a medium with the negative dispersion (when the phase velocity of linear waves decreases with the increasing wavenumber) as well as to a medium with the positive dispersion – the difference is only in the direction of the  $x$ -axis. Furthermore, for the convenience of an ad hoc study, we use various forms of the KdV equation.

The first solutions of the KdV equation were obtained numerically [1,93]. The studies showed that the equation can have two kinds of locally stationary solutions:

- (a) In the form of moving solitons; and
- (b) Of the type of periodic *cnoidal waves* (see below).

Later in 1967 [19] it was shown that the KdV equation is a completely integrable Hamiltonian system (see Sect. 1.2) and its soliton solution, found analytically for equation in the form (1.19), is given by [3]

$$u(t, x) = \frac{a^2}{2} \cosh^{-2} \left[ \frac{a}{2} (x - x_0 - a^2 t) \right],$$

---

<sup>2</sup> Note that in the case  $\theta = \pi/2$  and  $n_e = n_i = n_0$  (perpendicular propagation of the wave in a two-component plasma), we have  $\beta = v_A c^2 / 2\omega_{pe}^2$  since  $\omega_{pe} = \omega_{pi} \sqrt{m_i/m_e}$ .

where  $a^2$  is the amplitude of the soliton whose velocity is proportional to  $a^2$  and whose width is inversely proportional to the square root of the amplitude,  $1/a$ . For the periodic cnoidal wave, the solution  $u(t, x)$  can be written using Jacoby elliptic functions, namely, the elliptic cosine  $\text{cn}[f(x)]$  (note that the name “cnoidal” originates here). In the following, we do not consider the periodic cnoidal wave solutions.

Note that the KdV equation can have  $N$ -soliton solutions describing the dynamics of interactions (collisions) of  $N$  solitons. We assume that

$$u(t, x) = 2\partial_x^2 \ln F \quad (1.20)$$

(obtained as an exact solution using the IST method, see Sect. 1.2.1) and (following [94]) choose the function  $F$  as

$$F_N = \sum_{\bar{\mu}} \exp \left[ \sum_{i=1}^N \mu_i \xi_i + \sum_{1 \leq i < j}^N \mu_i \mu_j A_{ij} \right], \quad (1.21)$$

where the sum on  $\bar{\mu}$  is for all sets  $\mu_i$  (the element  $\mu_i$  can take a value 0 or 1,  $i = 1, \dots, N$ ). Furthermore,  $\xi_i = k_i(x - x_{0i} - k_i^2 t)$  and the factors  $A_{ij}$  are defined by

$$e^{A_{ij}} = \left( \frac{k_i - k_j}{k_i + k_j} \right)^2. \quad (1.22)$$

Thus we obtain the  $N$ -soliton solution of the KdV equation. For example, for  $N = 1$  we have  $F_1 = 1 + e^{\xi_1}$  from (1.21), and the solution is as that above with  $a = k_1$ ; for  $N = 2$  we have

$$F_2 = 1 + e^{\xi_1} + e^{\xi_2} + e^{\xi_1 + \xi_2 + A_{12}}, \quad (1.23)$$

where  $\xi_2 = -(k_2^2 - k_1^2)t + \xi_1$ , and substituting (1.23) into (1.20), we obtain the 2-soliton solution where the phase delay appearing as a result of the solitons' interaction is defined by the factor  $A_{12}$ .

To conclude this brief remark on the construction of the soliton solutions, we note that the choice of values of the constants  $x_{0i}$  is quite arbitrary. Thus, using the above direct method, we can also construct other classes of solutions. For example, choosing  $\exp k_1 x_{01} = -1$  in (1.21) for  $N = 1$ , we obtain a *singular solution*

$$u(t, x) = -\frac{k_1^2}{2} \sinh^{-2} \frac{k_1}{2} (x - k_1^2 t).$$

In the long-wavelength limit  $k_1 \rightarrow 0$ , we obtain the solution  $u = -2/x^2$  [26] which is the first representative of the class of the rational solutions of the KdV equation. Generally, by choosing proper phase constants in (1.21) we can obtain a non-trivial limit for any function  $F_N$ .

To obtain the criterion enabling us to distinguish solutions of the KdV equation into two classes (the soliton and non-soliton types of waves), Karpman formulated the *similarity principle* in 1966 [93]. Here, we consider it on

the basis of (1.18) with  $\alpha = 1$ . We set up the initial value problem, i.e., write the initial condition for the KdV equation as given by

$$u(0, x) = u_0 \varphi(x/l), \quad (1.24)$$

where  $u_0$  is the initial amplitude and  $l$  is the linear size of the initial disturbance. Changing  $u_0$  and  $l$ , we obtain a family of similar initial conditions characterized by the dimensionless function  $\varphi(x/l)$ . Introducing new variables

$$\eta = u/u_0, \quad \xi = x/l, \quad \text{and} \quad \tau = u_0 t/l, \quad (1.25)$$

we obtain from the KdV equation (1.18) with  $\alpha = 1$  and initial condition (1.24) the equation

$$\partial_\tau \eta + \eta \partial_\xi \eta + \sigma^{-2} \partial_\xi^3 \eta = 0, \quad (1.26)$$

where  $\eta(0, \xi) = \varphi(\xi)$  and

$$\sigma = l (u_0/\beta)^{1/2}. \quad (1.27)$$

It follows from (1.26) that solutions corresponding to the same value of  $\sigma$  and the same initial function  $\varphi(\xi)$  are similar. For solitons,

$$u(x) = u_0 \cosh^{-2} \left[ (u_0/12\beta)^{1/2} x \right], \quad (1.28)$$

we have

$$\sigma = \sigma_s = \sqrt{12}.$$

The parameter  $\sigma$  is, in fact, the index of nonlinearity of the problem, and  $\sigma_s$  is in some sense a characteristic value: as numerical simulations [93] demonstrated, for the same form of the initial function  $\varphi(\xi)$  in the cases  $\sigma \gg \sigma_s$  and  $\sigma \ll \sigma_s$ , qualitatively different solutions are observed. We study them in detail in the next sections (especially in Sect. 1.3.5) after we briefly consider other equations of the KdV-class.

### 1.1.3 Other (1+1)-Dimensional KdV-Class Equations

Other (1+1)-dimensional<sup>3</sup> KdV-class equations to be considered here are the linearized KdV equation, the Burgers equation and the Korteweg–de Vries–Burgers (KdVB) equation, as well as the generalized KdV equation with the higher order dispersion correction (Kawahara equation [84]) and terms taking into account dissipation and instability in a medium. Numerical solutions of these equations are given below in Sect. 1.3 after considering the analytical and numerical methods of integration of KdV-class equations.

---

<sup>3</sup> This terminology, often used in the mathematical literature, refers to the number of independent variables, namely, the time and the space coordinate in the present case.



**The linearized KdV Equation.** Linear approximation to (1.18) is given by the *linearized KdV equation*

$$\partial_t u + c_0 \partial_x u + \beta \partial_x^3 u = 0. \quad (1.29)$$

In the reference frame moving with the velocity  $c_0$  we obtain

$$\partial_t u + \beta \partial_x^3 u = 0. \quad (1.30)$$

The general solution of this equation expressed via the Airy function is [3]

$$u(t, x) = \pi^{-1/2} (3\beta t)^{-1/3} \int_{-\infty}^{\infty} \text{Ai} \left[ \frac{x - x'}{(3\beta t)^{1/3}} \right] u(0, x') dx', \quad (1.31)$$

where

$$\text{Ai}(z) = \frac{1}{\sqrt{\pi}} \int_0^{\infty} \cos \left( \frac{v^3}{3} + vz \right) dv \quad (1.32)$$

has the following asymptotics

$$\text{Ai}(z) = \begin{cases} (z^{-1/4}/2) \exp(-2z^{3/2}/3), & z \rightarrow \infty, \\ |z|^{-1/4} \cos \left( (2|z|^{3/2}/3) - \pi/4 \right), & z \rightarrow -\infty. \end{cases}$$

Although we are able to conclude on the solution's behavior from this general solution, it is difficult to see the change of dynamics of an initial disturbance (in the region of its localization) as a function of the dispersion parameter  $\beta$  since it is necessary to construct the corresponding Airy function in this case. Therefore numerical methods are better for the analysis of the structure and evolution of the solution of the linearized KdV equation (1.30). The results obtained numerically are given below in Sect. 1.3.

**The Burgers equation.** Consider the equation describing nonlinear waves in a medium with the “viscous” type of damping,

$$\partial_t u + u \partial_x u = \nu \partial_x^2 u. \quad (1.33)$$

This equation was obtained and analyzed by Burgers in 1940 [15] and is now called the *Burgers equation*. The general solution of this equation can also be obtained analytically. Namely, if

$$u = -2\nu \partial_x \ln \varphi(t, x), \quad (1.34)$$

for the function  $\varphi$  then one can obtain the heat conductivity (diffusion) equation

$$\partial_t \varphi = \nu \partial_x^2 \varphi.$$

In this case, the solution of the Burgers equation with the initial condition  $u(0, x) = \psi(x)$  can be written as (1.34), where [3]

$$\varphi(t, x) = \frac{1}{\sqrt{4\pi\nu t}} \int_{-\infty}^{\infty} \exp \left[ -\frac{(x - \eta)^2}{4\nu t} - \frac{1}{2\nu} \int_0^{\eta} \psi(\eta') d\eta' \right] d\eta.$$

However, some additional condition(s) need to be imposed for convergence of the integral on the right-hand side of this expression. In general, the structure of solution (1.34) is not that transparent and it is difficult to estimate its dynamics for various  $\nu$ . In this regard, it is helpful to integrate the Burgers equation numerically, and the corresponding results are also presented in Sect. 1.3.

## 1.2 Inverse Scattering Transform and Analytical Integration

In this section, we consider fundamentals of the theory of the inverse scattering transform (Sect. 1.2.1), the powerful method that enables us to obtain analytically general solutions of some classes of canonical nonlinear equations. On this basis, we approach the problem of (exact) analytical integration of the KdV equation in Sect. 1.2.2. In Sect. 1.2.3, we consider generalization of the Gelfand–Levitan–Marchenko integral equation for the purpose of possible separation of the study of the soliton and non-soliton parts of the solution. Finally, we consider the variational principle which practically enables us to separate the solutions (Sect. 1.2.4). The inverse scattering problem for the multidimensional cases is considered later in Chap. 3 (see Sect. 3.2).

### 1.2.1 Fundamentals of the Inverse Scattering Theory

The inverse scattering transform (IST) method in its classic form is a very convenient tool for solving the initial value (Cauchy) problem for nonlinear evolution equations. Note that when the Cauchy problem is solved on a class of functions decreasing sufficiently fast at infinity ( $u(\mathbf{r}) \rightarrow 0$  when  $|\mathbf{r}| \rightarrow \infty$ ), the *IST method* is as effective as the Fourier method for integration of linear partial differential equations with the constant coefficients (when the Fourier transform reduces the partial differential equation to an infinite set of ordinary linear differential equations for Fourier harmonics). When the equation's coefficients do not depend on the coordinates, the equations for the Fourier harmonics are independent and can be trivially integrated. The situation is similar when the IST method is applied. The mapping of the coefficient functions of a linear differential operator to the set of so-called “scattering data” plays the role of the Fourier transform here.

For example, the KdV equation is integrated with the help of the transition from the potential of the one-dimensional *Schrödinger equation*,

$$-\mathrm{d}_x^2 \psi + u(x)\psi = k^2 \psi,$$

to the *reflection coefficient*  $r(k)$  on this potential. As the potential  $u(x)$  evolves according to the KdV equation, the dependence of the reflection coefficient on time is trivial:

$$r(k, t) = r(k, 0) \exp(-8ik^3 t).$$

Thus, the problem of integrating the KdV equation is converted to the problem of reconstruction of the potential  $u(x)$  for the given reflection coefficient, i.e., the inverse of the (quantum) scattering problem.

Consider fundamental statements of the scattering theory for the one-dimensional *Sturm–Liouville operator* (*Schrödinger operator*),

$$\hat{L} = -d_x^2 + u(x),$$

on the (whole) real axis  $-\infty < x < \infty$ . We assume that the real potential  $u(x)$  is a sufficiently smooth function of  $x$  that turns to zero as  $|x| \rightarrow \infty$ . We consider the eigenvalue problem

$$\hat{L}\psi \equiv -d_x^2\psi + u(x)\psi = \lambda\psi, \quad (1.35)$$

where the eigenvalues  $\lambda = k^2$  is the (full) energy and  $k$  is the momentum of the system, on the class of (limited on the whole  $x$ -axis) functions  $\psi(x)$ . The spectrum of the operator  $\hat{L}$  consists of two parts, discrete and continuous, such that the *continuous spectrum* occupies the real half-axis  $\lambda > 0$  (real  $k$ ), and the eigenvalues of the *discrete spectrum* are negative (corresponding to the points of the imaginary axis  $k = i\kappa_n$ ,  $n = 1, 2, \dots, N$ ,  $\kappa_n > 0$ ).

Changing  $\lambda$  on the right-hand side of (1.35) to  $k^2$ , we write the equation defining the eigenfunctions as

$$-d_x^2\psi + u(x)\psi = k^2\psi. \quad (1.36)$$

First, consider the characteristics of the continuous spectrum. For every real  $k \neq 0$ , the set of solutions of (1.36) constitutes the two-dimensional linear space  $\mathbb{G}_k$ . We fix two bases in  $\mathbb{G}_k$ .

The first basis consists of solutions  $\psi_{1,2}(x, k)$  of (1.36) determined by the asymptotic conditions at  $+\infty$  in  $x$ :

$$\begin{cases} \psi_1(x, k) = e^{-ikx} + O(1), \\ \psi_2(x, k) = e^{ikx} + O(1), \end{cases} \quad x \rightarrow +\infty.$$

The second basis consists of solutions  $\varphi_{1,2}(x, k)$  determined by the analogous conditions at  $-\infty$ :

$$\begin{cases} \varphi_1(x, k) = e^{-ikx} + O(1), \\ \varphi_2(x, k) = e^{ikx} + O(1), \end{cases} \quad x \rightarrow -\infty.$$

Due to the real character (zero imaginary part) of the potential, we have

$$\varphi_1(x, k) = \varphi_2^*(x, k) \quad \text{and} \quad \psi_1(x, k) = \psi_2^*(x, k). \quad (1.37)$$

It is also obvious that

$$\varphi_1(x, k) = \varphi_2(x, -k) \quad \text{and} \quad \psi_1(x, k) = \psi_2(x, -k). \quad (1.38)$$

Vectors of either basis are the linear combination of vectors of the other:

$$\varphi_i(x, k) = \sum_{l=1,2} T_{il}(k) \psi_l(x, k), \quad i = 1, 2.$$

The matrix  $T(k)$ , introduced above, is called the *transition matrix*.<sup>4</sup> We have

$$T(k) = \begin{bmatrix} a(k) & b(k) \\ b^*(k) & a^*(k) \end{bmatrix}.$$

Omitting the indices 1 and 2 of the functions  $\varphi$  and  $\psi$ , we write

$$\varphi(x, k) = a(k)\psi(x, k) + b(k)\psi^*(x, k). \quad (1.39)$$

The Wronskian  $W(f_1, f_2) = f_1 d_x f_2 - f_2 d_x f_1$  of any pair of the solutions  $f_1$  and  $f_2$  of (1.36) does not depend on  $x$ . It is clear that  $W(\varphi, \varphi^*) = W(\psi, \psi^*) = 2ik$ . This relation together with (1.39) gives us

$$|a(k)|^2 - |b(k)|^2 = 1, \quad (1.40)$$

i.e., we see that the transition matrix is a unimodular one:  $\det T(k) = 1$ .

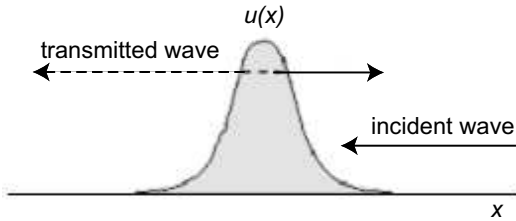


**Fig. 1.1.** Sketch of the scattering problem for a wave incident on the potential  $u(x)$

The functions  $a^{-1}(k)$  and  $b(k)a^{-1}(k)$  are the *transmission coefficient* and the *reflection coefficient*, respectively, of the wave incident to the potential  $u(x)$  from the right (see Fig. 1.1). In reality, the asymptote of the eigenfunction  $\varphi(x, k)/a(k)$ , see (1.39), for  $x \rightarrow +\infty$  is given by

$$a^{-1}\varphi(x, k) = e^{-ikx} + ba^{-1}e^{ikx} + O(1),$$

i.e., it is a superposition of the incident and reflected waves. At the other end of the  $x$ -axis we have

<sup>4</sup> Written as  $T(k) \equiv S(k) = \begin{bmatrix} s_{11}(k) & s_{12}(k) \\ s_{21}(k) & s_{22}(k) \end{bmatrix}$ , this matrix is often called the  $S$ -matrix or the scattering matrix.

$$a^{-1}\varphi(x, k) = a^{-1}e^{-ikx} + O(1),$$

i.e. only the transmitted wave propagates there. In other words,  $t(k) = a^{-1}(k)$  is the amplitude of the forward scattering and  $r(k) = b(k)a^{-1}(k)$  is the amplitude of the backward scattering. It follows from (1.40) that the scattering is unitary, i.e.,

$$|t(k)|^2 + |r(k)|^2 = 1.$$

An analysis of the analytic properties of the amplitude of the forward scattering on the physical sheet of the Riemann surface (we omit details here to save space) shows that (see Fig. 1.2)  $a(k)$  is an analytic function in the upper semi-plane of complex  $k$  and has simple zeros at the points  $k_n = i\kappa_n$ ,  $\kappa_n^2 = -\lambda_n$ ; in addition,  $a(k) \rightarrow 1$  for  $|k| \rightarrow \infty$ ,  $\text{Im } k \geq 0$ . These analytic properties of the diagonal elements of the transition matrix are principally important and, to a certain degree, universal. Analogous statements can be made in the scattering theory for other differential operators.

The *transition matrix*  $T(k)$  gives us comprehensive information on the *continuous spectrum* of the Schrödinger operator. The information on  $T(k)$  is fully contained in the reflection coefficient

$$r(k) = \frac{b(k)}{a(k)}, \quad (1.41)$$

that, in view of relations (1.37) and (1.38), can be determined only on the semi-axis  $k > 0$  since  $r(-k) = r^*(k)$ . From (1.40) we can easily obtain

$$|a(k)|^2 = \frac{1}{1 - |r(k)|^2}, \quad (1.42)$$

i.e., the modulus of the reflection coefficients uniquely defines  $|a(k)|$ . Knowing zeros of the analytic (in the upper semi-plane) function  $a(k)$ , it is possible to find the unique argument  $\arg[a(k)]$  by its modulus. Thus  $a(k)$  is reconstructed

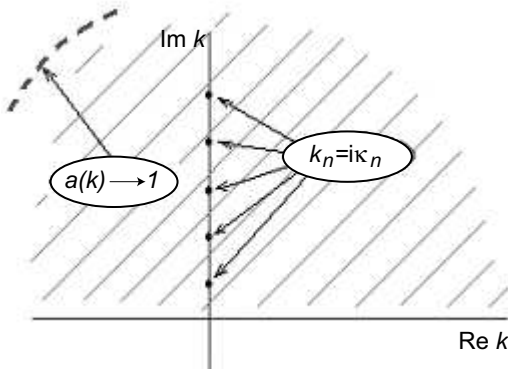


**Fig. 1.2.** Analytic properties of the amplitude of the forward scattering  $a(k)$

according to the modulus of the reflection coefficient, and the function  $b(k)$  is simply  $r(k)a(k)$ .

Consider now characteristics of the discrete spectrum of the *Sturm-Liouville operator* (*Schrödinger operator*) matching naturally the scattering characteristics. The eigenfunctions corresponding to the eigenvalue  $\lambda_n = -\kappa_n^2$  satisfy the equation

$$-d_x^2\psi + u(x)\psi = -\kappa_n^2\psi.$$

The discrete spectrum of the Schrödinger operator, as it is known, is simple: all solutions of this equation can be obtained from any one by multiplying it by a constant. At infinity, the eigenfunctions have the asymptotes

$$\psi \rightarrow c_{\pm} \exp(\mp \kappa_n x). \quad x \rightarrow \pm\infty.$$

Fix the eigenfunction  $\varphi^{(n)}(x)$  at  $-\infty$  in  $x$  by its asymptote

$$\varphi^{(n)}(x) = e^{\kappa_n x} + O(e^{\kappa_n x}).$$

When  $x \rightarrow +\infty$  the eigenfunctions are given by

$$\varphi^{(n)}(x) = b_n e^{-\kappa_n x} + O(e^{-\kappa_n x}); \quad (1.43)$$

obviously, they are real, and therefore the factors  $b_n$  are also real. If we arrange the eigenvalues  $\lambda_n$  in a usual way in order of increasing  $\lambda_n$  (i.e., decreasing  $\kappa_n$ ), namely,

$$\lambda_1 < \lambda_2 < \dots < \lambda_N < 0$$

(here,  $\lambda_1$  is the energy of the ground (basic) state of a quantum system and the corresponding function  $\varphi^{(1)}$  is the wave function of this state), then  $\varphi^{(1)}$  has no zeros and  $\varphi^{(n)}$  crosses zero exactly  $(n-1)$  times. Thus

$$b_n = (-1)^{n-1} |b_n|.$$

The positive quantities  $|b_n|$  consist additional (to the eigenvalues  $\lambda_n$ ) characteristics of the discrete spectrum. These characteristics together with the reflection coefficient  $r(k)$  and the set of eigenvalues  $\lambda_1, \lambda_2, \dots, \lambda_N$  fully determine the spectrum of problem (1.36). The set

$$S = \{r(k), \kappa_n, |b_n|, \quad n = 1, 2, \dots, N\}$$

is called the *scattering data*. Mapping  $u(x) \rightarrow S$  of potentials  $u(x)$  to the scattering data is uniquely reversible. The procedure of reconstruction of the potential  $u(x)$  on  $S$  is the subject of the inverse problem of the scattering theory.

The analytic properties of the special solutions of the Schrödinger equation introduced via the scattering data enable us to write the integral equations equivalent to (1.36) on the functions

$$\chi_+(x, k) = \varphi(x, k)e^{ikx} \quad \text{and} \quad \chi_-(x, k) = \psi(x, k)e^{-ikx}$$

using the Green's function. The function  $\chi_+(x, k)$  can be analytically continued to the upper semi-plane  $k$  (i.e. to  $\text{Im } k > 0$ ), and the function  $\chi_-(x, k)$  can be analytically continued to the lower semi-plane  $k$ . Thus for  $|k| \rightarrow \infty$  we have

$$\begin{aligned}\chi_+(x, k) &= 1 + \frac{1}{2ik} \int_{-\infty}^x u(x') dx' + O\left(\frac{1}{k^2}\right), \\ \chi_-(x, k) &= 1 + \frac{1}{2ik} \int_x^{\infty} u(x') dx' + O\left(\frac{1}{k^2}\right).\end{aligned}\quad (1.44)$$

For the Schrödinger operator, the most known form of the IST equation, i.e., of the equation describing the transition from the scattering data  $\mathbf{S}$  to the potential  $u(x)$ , is the *Gelfand–Levitan–Marchenko equation* (*GLM equation*). Now we are ready to obtain this equation. The procedure involves the following steps:

1. First of all, we note that Fourier transform of the function  $\chi_-(x, k)$  (analytic in the lower semi-plane  $k$ ) is cut off. Thus the function  $\chi_-(x, k)$  can always be written as

$$\chi_-(x, k) = 1 + \int_0^{\infty} \mathbf{A}(x, y) e^{-iky} dy.$$

2. For the function  $\psi(x, k)$ , this means that there is a function  $\mathbf{K}(x, y)$  such that

$$\psi(x, k) = e^{-ikx} + \int_x^{\infty} \mathbf{K}(x, y) e^{-iky} dy. \quad (1.45)$$

Obviously,  $\mathbf{K}(x, y) = \mathbf{A}(x, y - x)$ .

3. It follows from (1.45) that there exists a linear operator transforming the solution of Schrödinger equation with the zero potential (the plane wave solution  $e^{-ikx}$ ) to the solution of this equation with the potential  $u(x)$ . The function  $\mathbf{K}(x, y)$  is called the kernel of the transformation operator and it is real because  $\psi(x, -k) = \psi(x, k)$  for  $\text{Im } k = 0$ .
4. Consider now equality (1.39). We multiply it by ratio  $e^{-iky}/a(k)$  and integrate in all real  $k$ :

$$\begin{aligned}& \int_{-\infty}^{\infty} \left[ \frac{\varphi(x, k)}{a(k)} - \underline{e^{-ikx}} \right] e^{iky} dk \\ &= \int_{-\infty}^{\infty} \left[ \psi(x, k) - \underline{e^{-ikx}} + r(k) \psi^*(x, k) \right] e^{iky} dk.\end{aligned}\quad (1.46)$$

(Note that the underlined terms sum up to zero and they are introduced because of convenience of further transformations – in fact, we just added to the both sides of (1.39) the term  $a(k)e^{-ikx}$ ).

Calculation of the integral on the left-hand side of (1.46), taking into account that the function under the integral has, in the upper semi-plane, only a finite number of simple poles and decreases for  $|k| \rightarrow \infty$ , gives us

$$2\pi i \sum_{n=1}^N \frac{\varphi(x, i\kappa_n) e^{-\kappa_n y}}{a'(i\kappa_n)},$$

where  $a'$  is the  $k$ -derivative of the function  $a(k)$  for  $k = i\kappa_n$ . Taking into account (1.43), taking place for the discrete spectrum, which can be written as

$$\varphi(x, i\kappa_n) = b_n \psi^*(x, -i\kappa_n) = b_n \psi(x, -i\kappa_n) \quad (1.47)$$

(the functions  $\varphi$ ,  $\psi$  and  $\psi^*$  on the imaginary axis are obviously equivalent), and (1.45) for  $k = i\kappa_n$ ,  $n = 1, \dots, N$ , we obtain for the integral on the left-hand side of (1.46) the expression

$$2\pi i \sum_{n=1}^N \frac{b_n e^{-\kappa_n(x+y)}}{a'(i\kappa_n)} + 2\pi i \int_x^\infty \mathbf{K}(x, z) \sum_{n=1}^N \frac{b_n e^{-\kappa_n(z+y)}}{a'(i\kappa_n)} dz.$$

Substituting now formula (1.45) into the right-hand side of (1.46) and introducing the new notation,

$$\mathbf{F}(x) \equiv \sum_{n=1}^N \frac{b_n e^{-\kappa_n x}}{ia'(i\kappa_n)} + \frac{1}{2\pi} \int_{-\infty}^\infty r(k) e^{ikx} dk, \quad (1.48)$$

we obtain finally the *GLM equation* given by

$$\mathbf{K}(x, y) + \mathbf{F}(x + y) + \int_x^\infty \mathbf{K}(x, z) \mathbf{F}(z + y) dz = 0. \quad (1.49)$$

5. It follows from expression (1.45) that the asymptotic expansion for the function  $\chi_-(x, k)$  gives us

$$\chi_-(x, k) = 1 + \frac{1}{ik} \mathbf{K}(x, x) + O\left(\frac{1}{k^2}\right), \quad |k| \rightarrow \infty.$$

Comparing that with (1.44) we can express the potential  $u(x)$  by the kernel of the transformation operator

$$u(x) = -2d_x \mathbf{K}(x, x). \quad (1.50)$$

Thus, to determine the potential  $u(x)$ , it is necessary to solve the integral GLM equation, i.e., to obtain the kernel of the transformation operator via the scattering data fully contained in the function  $\mathbf{F}(x)$ , see (1.48). Now, having considered the fundamentals of the theory of scattering, we are able to proceed to the integration of the KdV equation using the IST method.



### 1.2.2 Integration of the KdV Equation Using the IST Method

Generally speaking, the *IST method* is the result of the outstanding observation by Gardner, Green, Kruskal and Miura who found [19] that solutions of the KdV equation can be associated with the potential of the Schrödinger equation.<sup>5</sup> Consider therefore the *Schrödinger equation* of the form

$$-d_x^2 f + u(x, t)f = k^2 f, \quad (1.51)$$

with the potential  $u(x, t)$  decreasing at  $x$ -infinity. We note that the function  $f$  can be a special solution of problem (1.51), e.g., with the asymptote

$$f(x, k) = e^{-ikx} + O(1), \quad x \rightarrow -\infty,$$

i.e., the solution  $\varphi(x, k)$  defined in the previous section.

If the potential  $u(x, t)$  depends on  $t$ , the function  $\varphi(x, k)$  also depends on  $t$  and then the scattering data become functions of  $t$ , too. The asymptote of  $\varphi(x, k)$  at  $x \rightarrow +\infty$  is then given by

$$\varphi(x, k, t) = a(k, t)e^{-ikx} + b(k, t)e^{ikx} + O(1). \quad (1.52)$$

In the case of an arbitrary dependence of  $u(x, t)$  on  $t$ , it is obviously not possible to find the general dependence of the scattering data on  $t$ . However, if  $u(x, t)$  changes in time as a solution of the KdV equation,  $\partial_t u - 6u\partial_x u + \partial_x^3 u = 0$ , then the “coefficient functions”  $a(k, t)$  and  $b(k, t)$  satisfy the Gardner–Green–Kruskal–Miura (GGKM) equations [19]

$$\dot{a}(k) = 0 \quad \text{and} \quad \dot{b}(k, t) = 8ik^3 b(k, t) \quad (1.53)$$

(here, the dot stands for the time derivative), and the dependence of  $\varphi(x, k, t)$  on  $t$  is given by the equation

$$\dot{\varphi}(x, k, t) = -\hat{A}\varphi(x, k, t) + 4ik^3 \varphi(x, k, t), \quad (1.54)$$

where the operator  $\hat{A}$  is

$$\hat{A} = 4d_x^3 - 3(ud_x + d_x u). \quad (1.55)$$

The inverse is also true: if the scattering data change in time as the GGKM-equation solutions then the potential  $u(x, t)$  (uniquely defined by them) satisfies the KdV equation. The simplest way to prove that is to note that the KdV equation is identical to the equation for the operators  $\hat{L} = -d_x^2 + u$  and  $\hat{A}$ :

$$\dot{\hat{L}} = [\hat{L}, \hat{A}] = \hat{L}\hat{A} - \hat{A}\hat{L}. \quad (1.56)$$

---

<sup>5</sup> Later this method was naturally extended to other evolution equations, e.g., the nonlinear Schrödinger (NLS) equation and the sin-Gordon equation.

Indeed,  $\hat{L}$  is just the multiplication operator  $\partial_t u$ , and the commutator  $[\hat{L}, \hat{A}]$ , as simple calculations demonstrate, is the multiplication operator  $6u\partial_x u - \partial_x^3 u$ , so that (1.56) coincides with the KdV equation,  $\partial_t u = 6u\partial_x u - \partial_x^3 u$ .

The representation of the evolution equations by (1.56) is called the *Lax representation* or Lax  $\hat{L}$ - $\hat{A}$  *pair* representation. With the help of the Lax representation it is not difficult to obtain for  $\varphi(x, k, t)$ , instead of (1.54), the following expression:

$$\dot{\varphi}(x, k, t) = \dot{a}e^{-ikx} + \dot{b}e^{ikx} = (-4d_x^3 + 4ik^3)(ae^{-ikx} + be^{ikx}),$$

which is equivalent to (1.53). Note that the functions  $a$  and  $b$  fully define the time dependence of the amplitude of the backward scattering

$$r(k, t) = r(k, 0)e^{8ik^3 t} = \frac{b(k, t)}{a(k, t)},$$

characterizing the continuous spectrum. Analogously we can solve the problem of the time evolution of the *scattering data*  $\kappa_n(t)$  and  $b_n(t)$  ( $n = 1, \dots, N$ ) for the discrete spectrum:

1. It follows from the first equation of (1.53) that  $i\kappa_n$  are the zeros of an analytic function  $a(k)$  independent of  $t$ , i.e.,  $\dot{\kappa}_n = 0$ ;
2. The dependence of  $b_n(t)$  can be obtained from (1.54) because by definition  $b_n$  is a factor in the asymptotic expansion of the function  $\varphi(x, i\kappa_n)$ , where

$$\varphi(x, i\kappa_n) = b_n(t)e^{-\kappa_n x} + O(e^{-\kappa_n x}), \quad x \rightarrow +\infty.$$

Substituting this asymptotic equation into (1.54), we obtain for  $k = i\kappa_n$  that  $\dot{b}_n = 8\kappa_n^3 b_n$ . Thus the time evolution of the *scattering data* is given by

**Table 1.1.** Scheme of solution of the initial value problem for the KdV equation

$u(x, 0)$	<b>I<sup>st</sup> stage</b>	Consists of calculation of the scattering data $S(0)$ , with the initial condition $u(x, t) _{t=0} = u(x, 0)$ , by finding the eigenfunctions of the Schrödinger operator with the potential $u(x, 0)$ .
$\Downarrow$		
$S(0)$	<b>II<sup>nd</sup> stage</b>	Involves solving the initial value problem in terms of the scattering data. The problem is trivial and its solution is given by (1.57).
$\Downarrow$		
$S(t)$	<b>III<sup>rd</sup> stage</b>	Takes place when using the GLM equation, the inverse problem is solved, i.e., the potential $u(x, t)$ in the Schrödinger operator is determined with $S(t)$ as the scattering data.
$\Downarrow$		
$u(x, t)$		Each stage implies solution of a <b>linear problem</b> only.

$$S(t) = \left\{ r(k, 0) e^{8ik^3 t}, \kappa_n, b_n e^{8\kappa_n^3 t}, n = 1, \dots, N \right\}. \quad (1.57)$$

We in fact integrated the KdV equation by means of the (implicit) change of the variables  $u(x) \rightarrow S$ . The inverse change  $S(t) \rightarrow u(x, t)$  gives us the solution of the KdV equation. Overall, the scheme of solution of the initial value problem for the KdV equation is given by Table 1.1. This scheme, despite the absence of a general analytical solution for both direct and inverse problems, enables us to find very important exact solutions of the KdV equation analytically, in particular, the one-soliton solution, and, in a more general case, the  $N$ -soliton solutions describing interactions (collisions) of KdV solitons.

### 1.2.3 Generalization of the GLM Equation

Consider the *Sturm–Liouville operator* (*Schrödinger operator*)

$$\hat{H}_j = -d_x^2 + u_j(x), \quad -\infty < x < \infty, \quad (1.58)$$

where  $u_j(x)$  is an element in the class of the scattering potentials. We suppose that  $u_j(x) \rightarrow 0$  (when  $|x| \rightarrow \infty$ ) sufficiently fast and, therefore, the standard theory of scattering is applicable. Then the spectrum of the operator  $\hat{H}_j$  consists of the continuous and discrete parts. The continuous spectrum occupies the real semi-axis  $\lambda = k^2 \geq 0$ , and the discrete spectrum consists of the negative  $\lambda = k^2 < 0$  non-degenerated point-like eigenvalues (we assume that their number is finite). We name the eigenfunctions of the continuous spectrum describing the scattering as  $\varphi_j(x, k)$ . They satisfy the *Schrödinger equation*

$$\hat{H}_j \varphi_j(x, k) = k^2 \varphi_j(x, k) \quad (1.59)$$

with the boundary conditions

$$\begin{cases} \varphi_j(x, k) = e^{-ikx} + ba^{-1}e^{ikx}, & x \rightarrow +\infty, \\ \varphi_j(x, k) = a^{-1}e^{-ikx}, & x \rightarrow -\infty. \end{cases} \quad (1.60)$$

Recall that  $t(k) = 1/a(k)$  is the amplitude of the forward scattering, and  $r(k) = b(k)/a(k)$  is the amplitude of the backward scattering for the potential  $u_j$ .

For the direct and inverse scattering problems, another set of eigenfunctions, namely, in the form of the *Jost function* satisfying the Schrödinger equation (1.59), but with another boundary condition,

$$\psi_j(x, k) = e^{ikx}, \quad x \rightarrow -\infty, \quad (1.61)$$

is also important (see Sect. 1.2.1). They are in fact pseudo-eigenfunctions because they are not quadratically integrated in general. The functions  $r(k)$ ,  $a^{-1}(k)$ , and  $\psi_j(x, k)$  satisfy the relations

$$\begin{cases} r(-k) = r^*(k), \\ a^{-1}(-k) = (a^{-1})^*(k), \\ \psi_j(x, k) = \psi_j^*(x, -k). \end{cases}$$

Note that the functions  $\psi_j$  and  $\psi_j^*$  are linearly independent. It is obvious that (see Sect. 1.2.1)

$$\varphi_j(x, k) = \psi_j(x, k) + r_j(k)\psi_j^*(x, k).$$

The discrete spectrum that the operator  $\hat{H}_j$  can have consists of a finite number of the point-like eigenvalues represented by

$$\lambda_{jn} = -\kappa_{jn}^2, \quad \kappa_{jn} > 0. \quad (1.62)$$

The corresponding eigenfunctions (note that they are true eigenfunctions in contrast to  $\psi_j$  which, as noted above, are “pseudo-eigenfunctions”) satisfy the Schrödinger equation

$$\hat{H}_j \varphi_{jn}(x) = \lambda_{jn} \varphi_{jn}(x) \quad (1.63)$$

together with the asymptotic condition

$$\lim_{x \rightarrow \pm\infty} \varphi_{jn}(x) = c_{\pm} e^{\mp \kappa_{jn} x}, \quad c_+ = b_n, \quad c_- = 1, \quad (1.64)$$

where the normalization factors are

$$|b_n| = \int_{-\infty}^{\infty} [\varphi_{jn}(x)]^2 dx. \quad (1.65)$$

In the inverse problem, we begin with the spectral data

$$S = \{r(k), \kappa_n, |b_n|, n = 1, 2, \dots, N\}$$

to obtain the scattering potential  $u_j(x)$  by using the *GLM equation* which was written in the previous section as

$$\mathbf{K}(x, y) + \mathbf{F}(x + y) + \int_x^\infty \mathbf{K}(x, z) \mathbf{F}(z + y) dz = 0, \quad (1.66)$$

where  $\mathbf{F}(x)$  is fully defined by the scattering data and the problem is, therefore, to determine the transform kernel  $\mathbf{K}(x, y)$ . The purpose of generalization of the GLM equation (1.66) is to introduce the “basic potential”  $u_m(x)$ . To do that we represent the potential  $u_j(x)$  as [95,96]

$$u_j(x) = u_m(x) + u_{jm}(x). \quad (1.67)$$

We assume that the spectral data  $S$  are known. The number of the point-like eigenvalues for  $u_m(x)$  is generally not equal to that of  $u_j(x)$ , i.e., the number of values of  $n$  in  $\kappa_{mn}$  is in general not equal to that in  $\kappa_{jn}$ . Using the GLM

equation (1.66) it is possible to obtain  $u_m(x)$  as well as the eigenfunctions  $\psi_m(x, k)$  and  $\varphi_{mn}(x)$ . Let  $\mathbf{K}_m(x, y)$  be the kernel of the GLM equation for  $u_m(x)$ . Then we can represent the “pseudo-eigenfunctions” of the *discrete spectrum*  $\varphi_{jn}(x)$  satisfying the *Schrödinger equation*

$$\hat{H}_m \ddot{\varphi}_{jn}(x) = -\kappa_{jn}^2 \ddot{\varphi}_{jn}(x)$$

as those given by

$$\ddot{\varphi}_{jn}(x) = e^{\kappa_{jn}x} + \int_{-\infty}^x \mathbf{K}_m(x, y) e^{\kappa_{jn}y} dy \quad (1.68)$$

(compare with (1.45) of the previous section). If the basic potential  $u_m(x)$  is a sufficiently short-range one then we can show that

$$\ddot{\varphi}_{jn}(x) = \psi_m(x, -i\kappa_{jn}), \quad (1.69)$$

where the right-hand side is obtained from  $\psi_m(x, k)$  through analytic continuation. The functions  $\ddot{\varphi}_{jn}(x)$ , as we noted above, are the “pseudo-eigenfunctions” of the operator  $\hat{H}_m$  since they are not quadratically integrated in general (although they satisfy the equation on the eigenfunctions of the operator  $\hat{H}_m$  with the discrete eigenvalue  $-\kappa_{jn}^2$ ). An exception is the case when  $\kappa_{jn} = \kappa_{ml}$  for some  $n$  and  $l$ . Then

$$\ddot{\varphi}_{jn}(x) = \varphi_{ml}(x) \quad (1.70)$$

and the pseudo-eigenfunction becomes the true eigenfunction for the operator  $\hat{H}_m$ .

Now we can write the generalized GLM equation. Introduce (instead of  $\mathbf{F}(x, y)$  in the GLM equation (1.49)) the function [95]

$$\begin{aligned} \Omega_{jm}(x, y) = & \frac{1}{2\pi} \int_{-\infty}^{\infty} \psi_m^*(x, k) [r_j(k) - r_m(k)] \psi_m^*(y, k) dk \\ & + \sum_n \frac{\ddot{\varphi}_{jn}(x) \ddot{\varphi}_{jn}(y)}{|b_{jn}|} - \sum_n \frac{\varphi_{mn}(x) \varphi_{mn}(y)}{|b_{jn}|} \end{aligned} \quad (1.71)$$

and require that the GLM kernel  $\mathbf{K}_{jm}(x, y)$  satisfies the one-dimensional *generalized GLM equation*, i.e.,

$$\mathbf{K}_{jm}(x, y) = -\Omega_{jm}(x, y) - \int_{-\infty}^x \mathbf{K}_{jm}(x, z) \Omega_{jm}(z, y) dz. \quad (1.72)$$

Then, as was shown in Sect. 1.2.1, we have

$$u_{jm}(x) = -2d_x \mathbf{K}_{jm}(x, x) \quad (1.73)$$

(compare the latter with (1.50)) and the functions  $\psi_j(x, k)$  and  $\varphi_{jn}(x)$  are determined by [95]

$$\psi_j(x, k) = \psi_m(x, k) + \int_{-\infty}^x \mathbf{K}_{jm}(x, y) \psi_m(y, k) dy, \quad (1.74)$$

and

$$\varphi_{jn}(x) = \ddot{\varphi}_{jn}(x) + \int_{-\infty}^x \mathbf{K}_{jm}(x, y) \ddot{\varphi}_{jn}(y) dy. \quad (1.75)$$

The function  $\Omega_{jm}(x, y)$ , as we see from (1.71), is fully determined by the scattering data. It is not difficult to see from the obtained expressions that if we take  $r_m(k) \equiv 0$  (where  $r_m(k)$  is the reflection coefficient for the basic potential) in the spectral data for  $u_m(x)$  and assume the absence of bound states (note that solitons appear as the result of the bound states), then we obtain  $u_m(x) \equiv 0$  and the generalized GLM equation (1.72) together with Eqs. (1.73)–(1.75) converts to the initial one-dimensional GLM equation with the properly defined functions  $\psi_j(x, k)$  and  $\varphi_{jn}(x)$ .

In the case of the KdV equation it is necessary to introduce the parameter  $t$  into the scattering data. We have

$$r_m(k, t) = r_m(k) e^{-i8k^3 t}, \quad |b_{mn}(t)| = |b_{mn}| e^{8\kappa_{mn}^3 t},$$

and

$$r_j(k, t) = r_j(k) e^{-i8k^3 t}, \quad |b_{jn}(t)| = |b_{jn}| e^{8\kappa_{jn}^3 t}.$$

Then the parameter  $t$  is included in the function  $\Omega_{jm}(x, y, t)$  (1.71) as well as the generalized GLM equation (1.72). In this case, instead of (1.73), we have

$$u_{jm}(x, t) = -2d_x \mathbf{K}_{jm}(x, x, t).$$

Thus,  $t$  is included in the potentials  $u_m(x, t)$ ,  $u_j(x, t)$ , and  $u_{jm}(x, t)$ , where the first two satisfy the *KdV equation*

$$\partial_t u + 6u \partial_x u + \partial_x^3 u = 0.$$

Instead of (1.67) where the basic potential  $u_m(x)$  is introduced, we now have

$$u_j(x, t) = u_m(x, t) + u_{jm}(x, t). \quad (1.76)$$

Thus we see that the generalized GLM equation allows us to separate  $u_m(x, t)$ , the soliton part of the solution of KdV equation, from  $u_{jm}(x, t)$ , the part corresponding to the *continuous spectrum*. When  $t \rightarrow \infty$ , because of the effect of dispersion,  $u_{jm}(x, t) \rightarrow 0$ , and the potential  $u(x, t)$  disintegrates into a (finite) number of solitons [96].

To be able to explain numerical results obtained for solitons of the KdV equation in the “non-stationary stage” [96] (see Sect. 1.3.5), consider here

correlations of the potentials  $u_{jm}(x, t)$  and  $u_m(x, t)$  in the region of small  $x$  for  $t \ll \infty$ , i.e., in the initial stage of dispersive spreading of the potential  $u_{jm}(x, t)$ . Choose in  $\Omega_{jm}(x, y, t)$  (1.71)

$$r_m(k) = 0, \quad |b_{mn}| = |b_{jn}|, \quad \text{and} \quad \kappa_{mn} = \kappa_{jn} \quad (1.77)$$

for all  $j$  (thereby we choose the necessary spectral data). Then  $u_m(x, t)$  is the soliton part of the solution (the non-reflective potential), and  $u_{jm}(x, t)$  is its non-soliton part corresponding to the continuous spectrum. The particular form of the solution is defined by the right-hand side of (1.71). The *Jost function*  $\psi_m(x, k)$  for the potential  $u_m(x, k)$  can be found explicitly but detailed analysis of (1.71) and (1.72) is difficult. Nevertheless, proceeding from the known asymptotic relations for  $\psi_m(x, k)$  for  $x \geq 0$  and accounting for the dependence of the reflection coefficient  $r_j(k, t)$  on  $t$ , we can conclude from the right-hand side of (1.71) (for the scattering data (1.77)) [96] the following:

1. A part of the solution determined by the potential  $u_{jm}(x, t)$  is an oscillating wave packet where the amplitude of the oscillations decreases in time due to dispersive spreading.
2. Since the “momentum”  $\int_{-\infty}^{\infty} u_j(x, t) dx$  conservation takes place for the KdV equation, we can write

$$\partial_t(u_j) + \partial_x[3u_j^2 + \partial_x^2(u_j)] = 0.$$

Substituting here the expression for  $u_j(x, t)$  from (1.76) and taking into account that  $u_j$  and  $u_m$  satisfy the KdV equation, we obtain [96]

$$u_m(x, t) \cdot u_{jm}(x, t) = \text{const.} \quad (1.78)$$

In the region of small  $x > 0$  when  $t \ll \infty$ , we see that the decrease of the potential  $u_{jm}(x, t)$  with time leads to the increase of the potential  $u_m(x, t)$ , corresponding to the soliton part (i.e., growth of the amplitudes of the solitons is observed) until the oscillating tail shifts as a whole to the region of negative  $x$ . With  $u_{jm}$  decreasing to zero in the region  $x > 0$ , the soliton parameters determined by the potential  $u_m$  tend to be constant values. For more detailed investigation of the behavior of the potential  $u_{jm}(x, t)$  corresponding to the non-soliton part of the solution (the non-reflective potential), one can use the variational principle first proposed for this purpose by Moses [95], as shown below.

### 1.2.4 The Variational Principle

Following Refs. [95,96] we introduce the functional

$$\mathbf{G}(\mathbf{N}, x) = -2 \left\{ \int_{-\infty}^x \mathbf{N}(x, y) dy \left[ 2\Omega(x, y) + \mathbf{N}(x, y) \right. \right. \\ \left. \left. + \int_{-\infty}^x \Omega(y, z) \mathbf{N}(x, z) dz \right] + \Omega(x, x) \right\}, \quad (1.79)$$

where  $\mathbf{N}(x, y)$  is the test function for the transformation kernel  $\mathbf{K}(x, y)$ . The *variational principle* states [95]:

**Theorem.** *The functional  $\mathbf{G}(\mathbf{N}, x)$  has an absolute maximum for all  $x$  if and only if  $\mathbf{N}(x, y) = \mathbf{K}(x, y)$ , i.e., the test function  $\mathbf{N}(x, y)$  is a solution of the generalized GLM equation, namely:*

$$\max_{x \in ]-\infty, \infty[} \{ \mathbf{G}(\mathbf{N}, x) \} = \mathbf{G}(\mathbf{K}, x), \quad \mathbf{N}(x, y) = \mathbf{K}(x, y).$$

*Besides, the absolute maximum of  $\mathbf{G}(\mathbf{K}, x)$  is equal to the area bound by the curve  $u_{jm}(x)$ :*

$$\int_{-\infty}^x u_{jm}(x') dx' = \mathbf{G}(\mathbf{K}, x).$$

This theorem allows us to calculate the potential  $u_{jm}(x)$  with increased accuracy. For such calculations, it is necessary: (a) to have an algorithm providing the test functions; and (b) to foresee the process allowing only increasing  $\mathbf{G}(\mathbf{N}, x)$  when testing the possible (test) functions in the computational program.

For example, for fixed  $x$  we can construct the histogram on  $y$  for  $\mathbf{N}(x, y)$ , which is varied in such a way that the functional  $\mathbf{G}(\mathbf{N}, x)$  is increased<sup>6</sup> (see Fig. 1.3). The same operation is repeated for the set of  $x$ -values for  $\mathbf{G}(\mathbf{N}, x)$  increasing from set to set. Furthermore, it is necessary to introduce time so that  $u_{jm}(x, t)$  is a part of the solution of the KdV equation corresponding to the continuous spectrum, and  $u_m(x, t)$  is its purely soliton part. Then one can obviously use the variational principle considered above. The functional now depends on  $x$  and  $t$ :  $\mathbf{G} = \mathbf{G}(\mathbf{N}, x, t)$ , and this corresponds to the continuous part of the spectrum, i.e., there should be the integral

<sup>6</sup> For example, one can construct an algorithm changing the height of each column of the histogram according to some procedure, then changing the widths of the columns using the best from the former histograms as the initial approximation.



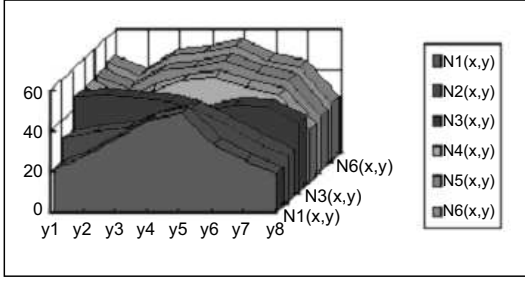


**Fig. 1.3.** Example of the histogram on  $y$  for  $\mathbf{N}(x, y)$  ( $x = \text{const}$ )

$$\int_{-\infty}^x u_{jm}(x', t) dx = \mathbf{G}(\mathbf{K}, x, t)$$

and there must be the maximum for all  $x$  and  $t$ , namely,

$$\max_{x \in [-\infty, \infty], 0 \leq t < \infty} \{\mathbf{G}(\mathbf{N}, x, t)\} = \mathbf{G}(\mathbf{K}, x, t), \quad \mathbf{N}(x, y, t) = \mathbf{K}(x, y, t).$$

Thus the variational principle provides new methods for computation of the continuous part of the wave solution, whereas the “classic” GLM equation is unable to separate the non-soliton part of the solution.

### 1.3 Numerical Integration of (1+1)-Dimensional KdV-Class Equations

As we already noted above, solutions of the KdV equation were first obtained numerically [1,93]. Later in 1967, Gardner, Green, Kruskal, and Miura [19] found the method to solve the KdV equation analytically using the IST method (see the previous section), and obtained exact solutions in the form of solitons.

However, even development of such powerful and effective analytical apparatus as the IST method does not remove the problem of numerical integration of the KdV equation as well as other equations in the KdV-class from the agenda because, first, it is not possible to obtain an analytical solution in its closed form using the IST method with arbitrary initial conditions, and, second, among the equations in the KdV-class there are models not integrated analytically (for example, KdV–Burgers equation (KdVB equation) or KdV equations with additional terms describing, for example, instability of some type in the medium). Therefore, developing numerical codes as well as setting up numerical experiments for this class of problems is highly important.

In this section, using the example of the KdV equation (1.18) we consider some difference schemes used for the numerical analysis and present numerical solutions obtained with their help. These schemes are also used to obtain solutions of other one-dimensional equations in the KdV-class, and some elements of these schemes will be further used (see Chap. 4) when studying

numerical methods of integration of the (1+2)- and (1+3)-dimensional problems.

### 1.3.1 Explicit Difference Schemes

For the KdV equation written in the form (1.18), we first consider the three-layer *explicit scheme with  $O(\tau^2, h^2)$  approximation*:

$$\begin{aligned} u_i^{n+1} = & u_i^{n-1} - \frac{\alpha\tau}{h} u_i^n (u_{i+1}^n - u_{i-1}^n) \\ & - \frac{\beta\tau}{h^3} (u_{i+2}^n - 2u_{i+1}^n + 2u_{i-1}^n - u_{i-2}^n). \end{aligned} \quad (1.80)$$

As we can see from the above difference equation, the scheme is realized on the 5-point template (Fig. 1.4). This scheme was used to obtain some of the first numerical solutions of the KdV equation in 1965–1968 [1,3,93]. Investigation of the stability of scheme (1.80) using Fourier analysis gives the

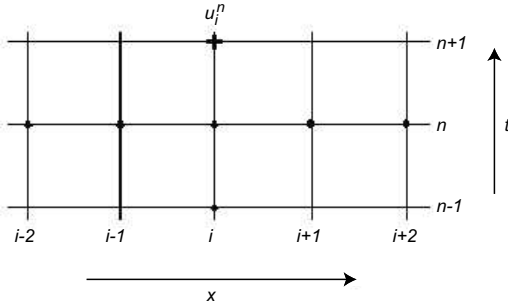


**Fig. 1.4.** Template for the difference scheme (1.80):  $n$  is the number of the time layer, and  $i$  is the number of the space layer

condition

$$\frac{\tau}{h} \max \left| \sin kh \left( \alpha u - \frac{4\beta}{h^2} \sin^2 \frac{kh}{2} \right) \right| \leq 1,$$

that is,

$$\frac{\tau}{h} \left( \alpha |u| + \frac{3\sqrt{3}\beta}{2h^2} \right) \leq 1,$$

or, for sufficiently small steps

$$\tau \leq \frac{2h^3}{3\sqrt{3}\beta} \cong 0.384 \frac{h^3}{\beta}. \quad (1.81)$$

Calculations demonstrate that this condition is quite accurate. For example, for  $\beta = 2 \times 10^{-4}$ ,  $\alpha = 1$ , and  $h = 0.01$ , the stability of the scheme is maintained for the time step  $\tau = 1.91 \times 10^{-3}$ , and the scheme is already

unstable when  $\tau = 1.93 \times 10^{-3}$ . Inequality (1.81) gives  $\tau = 1.92 \times 10^{-3}$  in this case.

Consider now the three-layer *explicit scheme with  $O(\tau^2, h^4)$  approximation*. Since here the approximation of the  $x$ -derivatives is used by finite differences of higher order than in the previous scheme, we introduce the 7-point template (Fig. 1.5). The scheme is given by

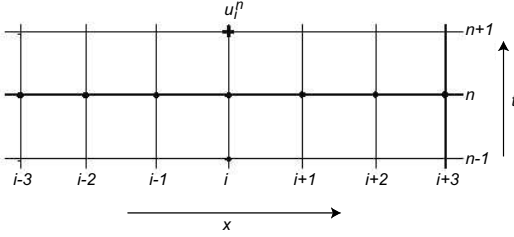


**Fig. 1.5.** Template for the difference scheme (1.82)

$$u_i^{n+1} = u_i^{n-1} + \frac{\alpha\tau}{6h} u_i^n (u_{i+2}^n - 8u_{i+1}^n + 8u_{i-1}^n - u_{i-2}^n) + \frac{\beta\tau}{4h^3} (u_{i+3}^n - 8u_{i+2}^n + 13u_{i+1}^n - 13u_{i-1}^n + 8u_{i-2}^n - u_{i-3}^n). \quad (1.82)$$

According to Fourier analysis, the scheme is stable when the condition on the steps  $\tau$  and  $h$ ,

$$\frac{\tau}{h} \max \left| \left[ \frac{4\beta}{h^2} \left( 1 + \sin^2 \frac{kh}{2} \right) \sin^2 \frac{kh}{2} - \left( 1 + \frac{2}{3} \sin^2 \frac{kh}{2} \right) \alpha u \right] \sin kh \right| \leq 1,$$

are satisfied. For sufficiently small steps  $h$ , we then obtain

$$\tau \leq \frac{108h^3}{(43 + 7\sqrt{73})\sqrt{10\sqrt{73} - 62\beta}} \cong 0.216 \frac{h^3}{\beta}. \quad (1.83)$$

A comparison of conditions (1.83) and (1.81) shows that the stability condition is more strict for the scheme with the higher approximation order.

### 1.3.2 Implicit Difference Schemes

For the example of an implicit difference scheme, consider first the *implicit scheme with  $O(\tau^2, h^4)$  approximation* [81,83]:

$$\begin{aligned}
\frac{u_i^{n+1} - u_i^n}{\tau} &= \frac{\alpha}{24h} \left[ u_i^n (u_{i+2}^{n+1} - 8u_{i+1}^{n+1} + 8u_{i-1}^{n+1} - u_{i-2}^{n+1}) \right. \\
&\quad \left. + u_i^{n+1} (u_{i+2}^n - 8u_{i+1}^n + 8u_{i-1}^n - u_{i-2}^n) \right] \\
&+ \frac{\beta}{16h^3} (u_{i+3}^{n+1} - 8u_{i+2}^{n+1} + 13u_{i+1}^{n+1} - 13u_{i-1}^{n+1} + 8u_{i-2}^{n+1} - u_{i-3}^{n+1} \\
&\quad + u_{i+3}^n - 8u_{i+2}^n + 13u_{i+1}^n - 13u_{i-1}^n + 8u_{i-2}^n - u_{i-3}^n). \quad (1.84)
\end{aligned}$$

Note that if we approximate the derivatives using the finite differences of another order, we obtain an implicit scheme of that approximation order. We see that in scheme (1.84), it is impossible to explicitly express the value of the function on the knot in the given time layer using the values of the function in the previous time layer (whence follows the name “implicit scheme”). Implicit schemes for sufficiently small steps  $h$  are absolutely stable and can be realized using the *sweep method*. In particular, for scheme (1.84), the method of the monotonous 7-point sweep (discussed below) is highly effective.

Let us represent (1.84) as

$$\begin{aligned}
&-a_0^1 u_3^n + a_0^2 u_2^n - a_0^3 u_1^n + a_0^4 u_0^n = h_0^n, & i = 0, \\
&-a_1^1 u_4^n + a_1^2 u_3^n - a_1^3 u_2^n + a_1^4 u_1^n - a_1^5 u_0^n = h_1^n, & i = 1, \\
&-a_2^1 u_5^n + a_2^2 u_4^n - a_2^3 u_3^n + a_2^4 u_2^n \\
&\quad - a_2^5 u_1^n + a_2^6 u_0^n = h_2^n, & i = 2, \\
&-a_i^1 u_{i+3}^n + a_i^2 u_{i+2}^n - a_i^3 u_{i+1}^n + a_i^4 u_i^n \\
&\quad - a_i^5 u_{i-1}^n + a_i^6 u_{i-2}^n - a_i^7 u_{i-3}^n = h_i^n, & 3 \leq i \leq N-3, \quad (1.85) \\
&a_{N-2}^2 u_N^n - a_{N-2}^3 u_{N-1}^n + a_{N-2}^4 u_{N-2}^n - a_{N-2}^5 u_{N-3}^n \\
&\quad + a_{N-2}^6 u_{N-4}^n - a_{N-2}^7 u_{N-5}^n = h_{N-2}^n, & i = N-2, \\
&-a_{N-1}^3 u_N^n + a_{N-1}^4 u_{N-1}^n - a_{N-1}^5 u_{N-2}^n \\
&\quad + a_{N-1}^6 u_{N-3}^n - a_{N-1}^7 u_{N-4}^n = h_{N-1}^n, & i = N-1, \\
&a_N^4 u_N^n - a_N^5 u_{N-1}^n + a_N^6 u_{N-2}^n - a_N^7 u_{N-3}^n = h_N^n, & i = N.
\end{aligned}$$

Here, for  $3 \leq i \leq N-3$ ,

$$h_i^n = -b_i (u_{i+3}^{n-1} - 8u_{i+2}^{n-1} + 13u_{i+1}^{n-1} - 13u_{i-1}^{n-1} + 8u_{i-2}^{n-1} - u_{i-3}^{n-1}) + u_i^{n-1},$$

and

$$\begin{aligned}
&n = 1, 2, \dots, N1, \quad b_i = a_i^7, \\
&a_i^1 = -\tau\beta/16h^3, \quad a_i^7 = -a_i^1, \\
&a_i^2 = (\tau/2h) (\beta/h^2 - \alpha u_i^{n-1}/12), \quad a_i^6 = -a_i^2, \quad (1.86) \\
&a_i^3 = (\tau/h) (\alpha u_i^{n-1}/3 - 13\beta/16h^2), \quad a_i^5 = -a_i^3, \\
&a_i^4 = 1 + (\alpha\tau/24h) (u_{i+2}^{n-1} - 8u_{i+1}^{n-1} + 8u_{i-1}^{n-1} - u_{i-2}^{n-1}),
\end{aligned}$$

where  $N1$  stands for the number of the time layers. The values  $h_i^n$  for  $i = 0, 1, 2$  and  $i = N-2, N-1, N$  are defined by

$$\begin{aligned}
h_0^n &= -a_0^1 u_3^{n-1} + a_0^2 u_2^{n-1} - a_0^3 u_1^{n-1} + a_0^4 u_0^{n-1}, \\
h_1^n &= -a_1^1 u_4^{n-1} + a_1^2 u_3^{n-1} - a_1^3 u_2^{n-1} + a_1^4 u_1^{n-1} - a_1^5 u_0^{n-1}, \\
h_2^n &= -a_2^1 u_5^{n-1} + a_2^2 u_4^{n-1} - a_2^3 u_3^{n-1} + a_2^4 u_2^{n-1} - a_2^5 u_1^{n-1} + a_2^6 u_0^{n-1}, \\
h_{N-2}^n &= a_{N-2}^2 u_N^{n-1} - a_{N-2}^3 u_{N-1}^{n-1} + a_{N-2}^4 u_{N-2}^{n-1} - a_{N-2}^5 u_{N-3}^{n-1} \\
&\quad + a_{N-2}^6 u_{N-4}^{n-1} - a_{N-2}^7 u_{N-5}^{n-1}, \\
h_{N-1}^n &= -a_{N-1}^3 u_N^{n-1} + a_{N-1}^4 u_{N-1}^{n-1} - a_{N-1}^5 u_{N-2}^{n-1} \\
&\quad + a_{N-1}^6 u_{N-3}^{n-1} - a_{N-1}^7 u_{N-4}^{n-1}, \\
h_N^n &= a_N^4 u_N^{n-1} - a_N^5 u_{N-1}^{n-1} + a_N^6 u_{N-2}^{n-1} - a_N^7 u_{N-3}^{n-1}.
\end{aligned} \tag{1.87}$$

The coefficients  $a_i^1, \dots, a_i^7$  for  $i = 0, 1, 2$  and  $i = N-2, N-1, N$  are obtained from the boundary conditions of the problem (see below in this section). The set (1.86) is solved using the monotonous 7-point sweep method; the procedure of developing the corresponding equations is analogous to the case of the 5-point sweep method considered in detail in numerous monographs and textbooks (see, for example, Ref. [97]). Therefore, here we present the algorithm in its final form [83,98].

The algorithm of monotonous 7-point *sweep method* for scheme (1.84) is based on the expressions

$$\begin{aligned}
\alpha_{i+1} &= (1/\Delta_i) \{a_i^3 - a_i^5 \beta_i + a_i^6 (\beta_i \alpha_{i-1} - \delta_{i-1}) - a_i^7 \\
&\quad \times [\alpha_{i-2} (\beta_i \alpha_{i-1} - \delta_{i-1}) - \beta_{i-2} \beta_i]\}, \quad \text{for } i = 3, 4, \dots, N-1; \\
\alpha_1 &= a_0^3/a_0^4, \quad \alpha_2 = (1/\Delta_1) (a_1^3 - a_1^5 \beta_1), \\
\alpha_3 &= (1/\Delta_2) [a_2^3 - a_2^5 \beta_2 + a_2^6 (\beta_2 \alpha_1 - \delta_1)]; \\
\beta_{i+1} &= \frac{1}{\Delta_i} [a_i^2 - a_i^5 \delta_i + a_i^6 \alpha_{i-1} \delta_i - a_i^7 (\alpha_{i-2} \alpha_{i-1} \delta_i - \beta_{i-2} \delta_i)], \\
&\quad \text{for } i = 3, 4, \dots, N-2; \\
\beta_1 &= a_0^2/a_0^4, \quad \beta_2 = (1/\Delta_1) (a_1^2 - a_1^5 \delta_1), \\
\beta_3 &= (1/\Delta_2) (a_2^2 - a_2^5 \delta_2 + a_2^6 \alpha_1 \delta_2); \\
\delta_{i+1} &= a_i^1/\Delta_i, \quad \text{for } i = 3, 4, \dots, N-3; \\
\delta_1 &= a_0^1/a_0^4, \quad \delta_2 = a_1^1/\Delta_1, \quad \delta_3 = a_2^1/\Delta_2; \\
\gamma_{i+1} &= \frac{1}{\Delta_i} \{a_i^5 \gamma_i - a_i^6 (\alpha_{i-1} \gamma_i + \gamma_{i-1}) + a_i^7 [\alpha_{i-2} (\alpha_{i-1} \gamma_i \\
&\quad + \gamma_{i-1}) - \beta_{i-2} \gamma_i + \gamma_{i-2}] - h_i\}, \quad \text{for } i = 3, 4, \dots, N; \\
\gamma_1 &= -h_0/a_0^4, \quad \gamma_2 = (1/\Delta_1) (-h_1 + a_1^5 \gamma_1), \\
\gamma_3 &= (1/\Delta_2) [-h_2 - a_2^6 (\alpha_1 \gamma_2 + \gamma_1) + a_2^5 \gamma_2]; \\
\Delta_i &= \{a_i^4 - a_i^5 \alpha_i + a_i^6 (\alpha_i \alpha_{i-1} - \beta_{i-1}) - a_i^7 [\alpha_{i-2} (\alpha_i \alpha_{i-1} \\
&\quad - \beta_{i-1}) - \beta_{i-2} \alpha_i + \delta_{i-2}]\}, \quad \text{for } i = 3, 4, \dots, N; \\
\Delta_1 &= a_1^4 - a_1^5 \alpha_1, \quad \Delta_2 = a_2^4 - a_2^5 \alpha_2 + a_2^6 (\alpha_2 \alpha_1 - \beta_1)
\end{aligned} \tag{1.88}$$

for the sweep coefficients  $\alpha_i$ ,  $\beta_i$ ,  $\gamma_i$ , and  $\delta_i$ . Then, using the expressions

$$\begin{aligned}
u_i &= \alpha_{i+1}u_{i+1} - \beta_{i+1}u_{i+2} + \delta_{i+1}u_{i+3} - \gamma_{i+1}, \\
&\quad \text{for } i = N-2, N-3, \dots, 0, \\
u_{N-1} &= \alpha_N u_N - \gamma_N, \quad u_N = -\gamma_{N+1},
\end{aligned} \tag{1.89}$$

we obtain the unknown quantities  $u_i$  one after another. Note that the sweep coefficients  $\alpha_i$  and  $\beta_i$  in (1.89) and (1.89) should not be mixed up with the coefficients  $\alpha$  and  $\beta$  of the original differential problem (1.18).

It is well known that the implicit difference schemes, theoretically, are absolutely stable. In our case of the nonlinear equation, however, the function  $u_i$  is included into the expressions for  $a_i$  (1.87). Therefore there are limitations on the correctness of the algorithm. In particular, the algorithm of the monotonous sweep method is correct when the following conditions are fulfilled [83,98]:

$$\begin{aligned}
|a_i^7| &> 0, & 3 \leq i \leq N; & & |a_i^6| &> 0, & 2 \leq i \leq N; \\
|a_i^5| &> 0, & 1 \leq i \leq N; & & |a_i^3| &> 0, & 0 \leq i \leq N-1; \\
|a_i^2| &> 0, & 0 \leq i \leq N-2; & & |a_i^1| &> 0, & 0 \leq i \leq N-3;
\end{aligned} \tag{1.90}$$

and

$$\begin{aligned}
|a_0^4| &\geq |a_0^3| + |a_0^2| + |a_0^1|, & |a_1^4| &\geq |a_1^5| + |a_1^3| + |a_1^2| + |a_1^1|, \\
|a_2^4| &\geq |a_2^5| + |a_2^6| + |a_2^3| + |a_2^2| + |a_2^1|, \\
|a_N^4| &\geq |a_N^5| + |a_N^6| + |a_N^7|, \\
|a_{N-1}^4| &\geq |a_{N-1}^3| + |a_{N-1}^5| + |a_{N-1}^6| + |a_{N-1}^7|, \\
|a_{N-2}^4| &\geq |a_{N-2}^2| + |a_{N-2}^3| + |a_{N-2}^5| + |a_{N-2}^6| + |a_{N-2}^7|, \\
|a_i^4| &\geq |a_i^1| + |a_i^2| + |a_i^3| + |a_i^5| + |a_i^6| + |a_i^7|, & 3 \leq i \leq N-3.
\end{aligned} \tag{1.91}$$

These conditions impose restrictions on KdV equation (1.18). Indeed, for  $3 \leq i \leq N-3$ , we have to satisfy the conditions given by

$$u_i^{n-1} \neq \frac{12\beta}{\alpha h^2} \quad \text{and} \quad u_i^{n-1} \neq \frac{39}{16\alpha h^2}. \tag{1.92}$$

These inequalities are satisfied for a sufficiently small step  $h \leq 0.2$ . Also, the last inequality of (1.92) should be satisfied for the coefficients (1.87). If the wave amplitude  $u_i^{n-1} \leq 30$  (i.e., it changes within reasonable limits), then

$$|a_i^4| \geq \frac{\tau}{4h} \left( \frac{11\beta}{h^2} - 3\alpha u_i^{n-1} \right). \tag{1.93}$$

Furthermore, if the following inequality is satisfied for a sufficiently smooth function  $u^{n-1}$ :

$$\frac{\alpha\tau}{24h} (u_{i-2}^{n-1} - 8u_{i-1}^{n-1} + 8u_{i+1}^{n-1} - u_{i+2}^{n-1}) \leq 1, \tag{1.94}$$

then follows the restriction [81,83,98]

$$\tau \leq 4h \left[ \frac{\alpha}{6} (u_{i-2}^{n-1} - 8u_{i-1}^{n-1} - 18u_i^{n-1} + 8u_{i+1}^{n-1} - u_{i+2}^{n-1}) + \frac{11\beta}{h^2} \right]^{-1} \cong \frac{4h}{3|\alpha u|}, \quad (1.95)$$

where  $u = \max_{i,n} |u_i^n|$ , that should be taken into account in calculations. In reality, as numerical simulations demonstrate, the given restriction on the time step is too strict since the adequate accuracy of the solution has been observed already for  $h = 0.1$  and  $\tau = 0.0025$ . For  $i = 0, 1, 2$  and  $i = N - 2, N - 1, N$ , in order to satisfy the conditions in (1.91), it is sufficient to choose proper boundary conditions, as described in the next section.

Consider now another *implicit scheme with  $O(\tau^2, h^2)$  approximation*:

$$\begin{aligned} \frac{u_i^{n+1} - u_i^n}{\tau} + \frac{\alpha}{4h} [u_i^n (u_{i+1}^{n+1} - u_{i-1}^{n+1}) + u_i^{n+1} (u_{i+1}^n - u_{i-1}^n)] \\ + \frac{\beta}{4h^3} (u_{i+2}^{n+1} - 2u_{i+1}^{n+1} + 2u_{i-1}^{n+1} - u_{i-2}^{n+1} \\ + u_{i+2}^n - 2u_{i+1}^n + 2u_{i-1}^n - u_{i-2}^n) = 0. \end{aligned} \quad (1.96)$$

Analogously to what was done for the scheme (1.84), we represent (1.96) as

$$\begin{aligned} a_0^1 u_2^n - a_0^2 u_1^n + a_0^3 u_0^n &= h_0^n, & i = 0, \\ a_1^1 u_3^n - a_1^2 u_2^n + a_1^3 u_1^n - a_1^4 u_0^n &= h_1^n, & i = 1, \\ a_i^1 u_{i+2}^n - a_i^2 u_{i+1}^n + a_i^3 u_i^n - a_i^4 u_{i-1}^n \\ &\quad + a_i^5 u_{i-2}^n = h_i^n, & 2 \leq i \leq N-2, \\ -a_{N-1}^2 u_N^n + a_{N-1}^3 u_{N-1}^n - a_{N-1}^4 u_{N-2}^n \\ &\quad + a_{N-1}^5 u_{N-3}^n = h_{N-1}^n, & i = N-1, \\ a_N^3 u_N^n - a_N^4 u_{N-1}^n + a_N^5 u_{N-2}^n &= h_N^n, & i = N. \end{aligned} \quad (1.97)$$

Here, for  $2 \leq i \leq N-2$ , we have

$$\begin{aligned} h_i^n &= (\tau/4h^3) (u_{i+2}^{n-1} - 2u_{i+1}^{n-1} + 2u_{i-1}^{n-1} - u_{i-2}^{n-1}) + u_i^{n-1}, \\ a_i^1 &= -\tau\beta/4h^3, & a_i^5 &= -a_i^1, \\ a_i^2 &= (\tau/4h) (\alpha u_i^{n-1} - 2\beta/h^2), & a_i^4 &= -a_i^2, \\ a_i^3 &= 1 + (\alpha\tau/4h) (u_{i+1}^{n-1} - u_{i-1}^{n-1}). \end{aligned} \quad (1.98)$$

For  $i = 0, 1$  and  $i = N-1, N$  in (1.98) we have

$$\begin{aligned} h_0^n &= a_0^1 u_2^{n-1} - a_0^2 u_1^{n-1} + a_0^3 u_0^{n-1}, \\ h_1^n &= a_1^1 u_3^{n-1} - a_1^2 u_2^{n-1} + a_1^3 u_1^{n-1} - a_1^4 u_0^{n-1}, \\ h_{N-1}^n &= -a_{N-1}^2 u_N^{n-1} + a_{N-1}^3 u_{N-1}^{n-1} - a_{N-1}^4 u_{N-2}^{n-1} + a_{N-1}^5 u_{N-3}^{n-1}, \\ h_N^n &= a_N^3 u_N^{n-1} - a_N^4 u_{N-1}^{n-1} + a_N^5 u_{N-2}^{n-1}. \end{aligned}$$

The coefficients  $a_i^1, \dots, a_i^5$  are determined by boundary conditions of the problem (see the next section). The set (1.98) can be effectively solved using the non-monotonous *sweep method*. We consider here neither the non-monotonous 5-point sweep method nor the final calculation expressions since

there are plenty of monographs and textbooks devoted to realization of various sorts of non-monotonous sweep methods. Here, we only note that the scheme (1.96) is correct under the condition that the matrix  $A$  of the set (1.98) is non-degenerated, i.e.,  $\det A \neq 0$ .

Thus we considered here some examples of explicit and implicit difference schemes constructed directly for the KdV equation. Some remarks regarding their adaptation to other KdV-class equations as well as the problem of boundary conditions are given below in the next section.

### 1.3.3 Remarks on Numerical Integration

1. In the case when the study of KdV-class equations involves some sort of an additional term, this term must be included into the difference schemes considered above with the appropriate order of approximation of the derivative. For example, if we investigate the KdVB equation with the term (on the right-hand side of the equation) describing wave damping as a result of a dissipative process in the medium,  $\nu \partial_x^2 u$ , it is necessary to include that term into the difference scheme with approximation of the appropriate order. For the scheme (1.80) this term is given by

$$\frac{2\nu\tau}{h^2} (u_{i+1}^n - 2u_i^n + u_{i-1}^n). \quad (1.99)$$

2. If some term is absent in the considered equation (as compared to the KdV equation) then it is sufficient to assume in the difference scheme that the corresponding coefficient equals zero (e.g., in the classic Burgers equation when  $\beta = 0$ ; of course, in this case it is still necessary to include the term (1.99) in the right-hand side of the difference equation. Thus, difference schemes (1.80), (1.82), (1.84) and (1.96) are general (in a certain sense) for the whole class of (1+1)-dimensional equations of the KdV type. Below, when presenting numerical methods for multidimensional equations (Sects. 3.1 and 4.3) we will also see that the schemes considered above are used there as their inalienable elements.
3. This remark is related to the boundary conditions of the problem. We note that although we solve the initial value problem for all presented cases, we should still impose constraints at the boundaries of the one-dimensional grid because of the limits of the region of numerical integration, i.e., the problem acquires features of the initial-boundary problem. Naturally, the difference derivatives in the schemes must be defined for  $i = 0, 1, 2$  and  $i = N - 2, N - 1, N$ . In this case, terms approximating the function  $u$  at the points corresponding to the limits of the integration region (where the function  $u$  is not defined) on the  $x$ -axis, appear in these schemes; accordingly, it is necessary to impose some conditions defining the function at these points. Here, different variants are possible, and the following discusses two possibilities most often used.



In the case when the initial condition  $u(0, x) = \psi(x)$  has the asymptotics  $|\psi(x)| \rightarrow 0$  for  $|x| \rightarrow \infty$  (tending to zero sufficiently fast with the increasing modulus  $x$ , e.g., exponentially where  $\psi(x) \sim \exp(-x^2)$  for  $|x| \rightarrow \infty$ ), we can use on the boundaries of the integration region the so-called zero boundary conditions

$$u(t, x) = \partial_x u(t, x) = \partial_x^2 u(t, x) = \partial_x^3 u(t, x) = 0.$$

If the condition on the (space) localization of the function  $\psi(x)$  defining the initial condition does not take place, the boundary conditions become more complex. For example, when the initial condition is  $\psi(x) = a \cos(mx + \varphi)$ , the periodic boundary conditions are usually used (they are given here for the grid  $i = 0, 1, \dots, N$ ):

$$\begin{cases} u_{N+1} = u_1, & u_{N+2} = u_2, & u_{N+3} = u_3, \\ u_{-1} = u_{N-1}, & u_{-2} = u_{N-2}, & u_{-3} = u_{N-3}. \end{cases}$$

In other cases, especially when solutions have more complex asymptotics with a slow tendency of the function  $u$  approaching zero at infinity, we can also use other boundary conditions. For example, the condition of the “total absorption” at the boundary or the impedance boundary condition of the Leontovich type is often used for simulations of more complex multidimensional evolution equations (see Sect. 4.3.2 for details).

Having considered various methods and schemes of numerical approach to the integration of (1+1)-dimensional KdV-class equations based on the finite-difference approximation of the derivatives, we now discuss their characteristics related to the calculation’s accuracy and productivity, in terms of the time expenses and demands on the computer memory. After that we can consider numerical solutions obtained by use of these schemes.

### 1.3.4 Test of Numerical Methods, Their Comparative Characteristics, and Use

To test the above difference schemes (1.80), (1.82), (1.84), and (1.96), we investigate their characteristics related to integration in the space coordinate  $x$ . As an initial condition we use the exact solution of the KdV equation

$$u_0(x) = \frac{3v}{\alpha} \cosh^{-2} \left[ \frac{\sqrt{v}}{2\beta} (x - x_0) \right],$$

where we choose  $v = \alpha = 6$  and  $\beta = 1$ . The control of the accuracy for all time layers is fulfilled by a comparison of the numerical solution with the above exact (analytical) solution. At each time step  $\tau$ , we calculate the relative mean deviation  $\varepsilon$ ,

$$\varepsilon = \frac{|u_\tau^{\text{num}} - u_\tau^{\text{exact}}|}{u_\tau^{\text{exact}}},$$

as well as the mean-square-root deviation of the numerical solution from the exact one,

$$s = \left[ \frac{1}{N} \sum_{i=1}^N \left| (u_i^{\text{num}})^2 - (u_i^{\text{exact}})^2 \right| \right]^{1/2}.$$

For example, for  $t = 0.4$  (the soliton is near the boundary of the integration region) the scheme (1.84) with  $h = 0.1$  and  $\tau = 0.0025$  gives us

$$\varepsilon = 6.38775 \times 10^{-3} \quad \text{and} \quad s = 1.74663 \times 10^{-4}.$$

This result is quite acceptable and is approximately on an order of magnitude better than the corresponding results for schemes proposed for the solution of the KdV equation in Refs. [79,93].

Comparative analysis of the results of numerical calculation employing the difference schemes (1.80), (1.82), (1.84), and (1.96) allows us to make the following conclusions. The schemes (1.82) and (1.84) naturally demonstrate the best accuracy characteristics. Conditions on the time grid step for these schemes are approximately the same and are less restrictive than those for scheme (1.80). Better possibilities to choose the time step in scheme (1.96) allow us to considerably decrease the necessary computer time as compared to other schemes. Obviously, the implicit schemes (1.84) and (1.96) have another advantage over the explicit schemes (1.80) and (1.82), viz., their two-layer structure ensures less requirements to the computer memory resources. For the same time steps  $\tau$  as in the implicit schemes, explicit schemes (1.80) and (1.82) are more preferable because of their lesser time expenses. Their three-layer structure, however, imposes severe requirements on the computer memory resources. These schemes can be effectively used for calculations on small time scales in the investigation of evolution of the initial condition at the “non-stationary stage” when there is a “birth” and the subsequent formation of locally stationary objects – solitons (see the next section).

### 1.3.5 Numerical Solutions of Some KdV-Class Equations

Consider now numerically obtained solutions of the KdV equation as well as some other equations in the KdV class. We begin with the linearized KdV equation (1.30) and Burgers equation (1.33) considered in Sect. 1.1. Although exact analytical solutions can be found for these equations, see (1.31) and (1.34), they are not transparent and are not convenient for detailed analysis of the dynamics of an initial disturbance.

For the fast decreasing initial disturbance for  $|x| \rightarrow \infty$ , numerical integration of *linearized KdV equation* (1.30) results in the following. The local wave number is given by

$$k(x, t) = \left| \frac{x}{3\beta t} \right|^{1/2},$$

and the local frequency is defined by  $\omega = -\beta k^3$ , as can be seen from the dispersion law for the linearized KdV equation. Evolution of the single initial disturbance

$$u(0, x) = u_0 \exp(-x^2/l^2) \quad (1.100)$$

(here,  $u_0$  and  $l$  are arbitrary parameters determined by the convenience of numerical calculation for a particular size of the region of the numerical integration) leads to formation of the oscillating wave packet shown in Fig. 1.6. In the case where  $\beta > 0$ , the “fast” oscillations are in the region  $x < 0$ ,

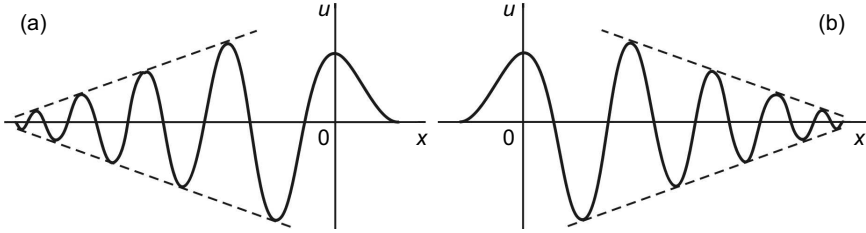


**Fig. 1.6.** Numerical solution of the linearized KdV equation. **a.**  $\beta > 0$  **b.**  $\beta < 0$

i.e., the short wavelength oscillations fall behind the large wavelength ones. If  $\beta < 0$  (note that it is generally easy to convert equation (1.30) with  $\beta < 0$  to the equation with  $\beta > 0$  by changing  $x \rightarrow -x$ ), the fast oscillations are in the region  $x > 0$ , i.e. the short wavelength waves are propagating forward. Thus the change  $x \rightarrow -x$  is equivalent to the change of the dispersion sign.

For numerical integration of the *Burgers equation* (1.33), we consider evolution of the initial disturbance  $u(0, x) = \psi(x)$  decreasing at  $|x| \rightarrow \infty$ . Following Ref. [3] we assume that

$$\int_{-\infty}^{\infty} \psi(x) dx = C < \infty, \quad (1.101)$$

and the profile of the initial condition can be arbitrary in other respects. We note only that for any  $t$  [3]

$$\int_{-\infty}^{\infty} u(t, x) dx = \int_{-\infty}^{\infty} u(0, x) dx = C;$$

this is easy to prove by writing the Burgers equation in the divergence form,

$$\partial_t u + \partial_x \left( \frac{1}{2} u^2 - \nu \partial_x u \right) = 0,$$

and then integrating both parts in  $x$  from  $-\infty$  to  $+\infty$ . Thus, the area bound by the function  $\psi(x)$  does not vary with time, i.e., it is the integral of motion.

Consider now the results of numerical simulations of the *Burgers equation*. Choosing for simplicity of numerical realization of the algorithm (the simplicity of the boundary conditions), the initial condition in the form of the single disturbance (1.100) as in the case of the linearized KdV equation, we obtain for large  $t$  the result presented in Fig. 1.7. For  $\nu \rightarrow 0$  (see curve 1

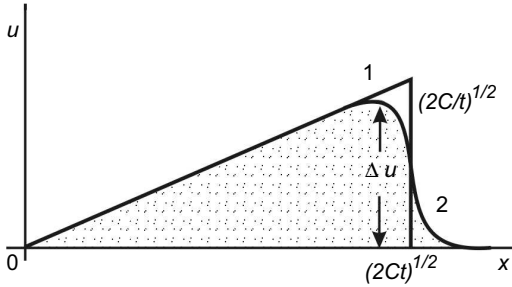


**Fig. 1.7.** Numerical solution of Burgers equation. Curve 1 corresponds to  $\nu = 0.0001$ , curve 2 corresponds to  $\nu = 0.1$ .

in Fig. 1.7), the profile of the solution is a triangle with the shock wave structure at its front. The jump of  $u$  at the shock wave is  $\sqrt{2C/t}$ , i.e., it decreases as the (inverse) square root of time; the basis (width) of the profile, on the contrary, increases as the square root of time, so the area of the profile is a constant equal to  $C$ .

For finite  $\nu$  (see curve 2 in Fig. 1.7), we obtain another solution, namely, the stationary wave traveling (without deformation) with a constant velocity  $w$ :

$$u = f(x - wt).$$

The jump of the wave,  $\Delta u$ , and the width of the transition region,  $\delta = 2\nu/\Delta u$ , are determined by the parameter  $\nu$  of the problem, i.e., by the dissipation factor defining the level of damping. We note that for  $\nu \rightarrow 0$  the parameter  $\delta$  also tends to zero, and in this limit we come again to the solution of type (a) of Fig. 1.7.

The results shown in Fig. 1.7 correspond to the case  $C > 0$ , i.e., when the area of the profile of the initial perturbation is positive. If  $C < 0$  then the change (in the Burgers equation)  $u \rightarrow -u$ ,  $x \rightarrow -x$ , and  $t \rightarrow -t$  allows us to return to the solutions considered above.

We consider now numerical solutions of the KdV equation itself, and also discuss, in general, the influence on the structure and dynamics of its solutions of the terms taking into account dissipation and instability<sup>7</sup>. For the analysis of numerical solutions we use the similarity principle formulated above in Sect. 1.1. Consider solutions of (1.11) corresponding to the most typical initial disturbances decreasing for  $|x| \rightarrow \infty$ . The evolution of disturbances of a

<sup>7</sup> Sections 2.1 and 2.2 below are specially devoted to detailed investigation of this problem.

similar type within the limits of the KdV model was studied numerically for the first time by Berezin and Karpman in 1966 [93].

Choosing the initial disturbance as a single pulse (1.100), we consider the dependence (for this initial condition) of the character of solutions on the parameter

$$\sigma = l \left( \frac{u_0}{\beta} \right)^{1/2}$$

(see (1.18) of Sect. 1.1). Numerical experiments of Ref. [93] (also repeated by us when testing the numerical schemes for more complicated generalized equations, see Chap. 4) show that for the sufficiently large  $\sigma \gg \sigma_s = \sqrt{12}$ , the initial wave pulse practically fully disintegrates with its evolution into individual solitons – see Fig. 1.8 (in addition to the solitons, an oscillating tail is also formed as the wave packet of a small amplitude). We note that solutions of the same type was obtained by Zabusky and Kruskal in 1965 [1] for the periodical initial condition  $u(0, x) = \cos(\pi x)$ . It follows from numerical

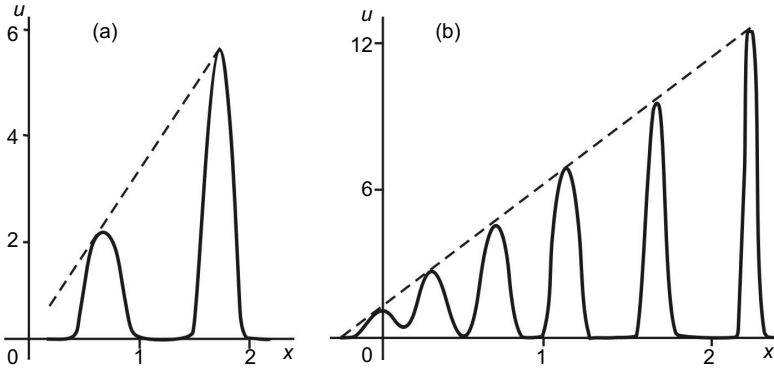


**Fig. 1.8.** Numerical solution of KdV equation for  $\beta > 0$ . **a.**  $\sigma = 5.9$ ; **b.**  $\sigma = 16.5$

calculations that the initial condition (1.100):

- for  $4 < \sigma < 7$ , decays into 2 solitons,
- for  $7 < \sigma < 11$ , decays into 3 solitons,
- for  $\sigma \sim 11$ , decays into 4 solitons,
- for  $\sigma \sim 16$ , decays into 6 solitons,

i.e., with increasing  $\sigma$  (decreasing  $\beta$ ) the corresponding initial disturbance decays into a growing number of solitons. This is clear because the decrease of the dispersion parameter  $\beta$  corresponds to the increasing role of nonlinear effects as related to the dispersion effects. We note that in the evolution of the solution, the integral

$$\int_{-\infty}^{\infty} u(t, x) dx$$

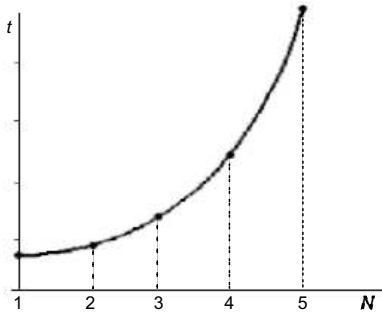


**Fig. 1.9.** Duration of the stage of the “non-stationary” evolution as a function of the number of the KdV soliton

is conserved, i.e. it is the integral of motion.

The evolution of an initial disturbance in the case when  $\sigma \gg \sigma_s$  has two stages which can be conditionally defined as:

1. The “non-stationary stage” corresponding to decay of the initial disturbance and to formation of individual solitons, i.e., solitary structures with the unchanging shape propagating with the constant velocities and amplitudes.
2. The stage of the stationary evolution, i.e. propagation of the solitons as stable solitary wave structures.

Up till 1985 practically all analytical and numerical investigations (constructions of exact solutions, investigations of collisional dynamics of solitons, etc.) were primarily limited to studies of the solutions on the second stage of the evolution, i.e., studies of the evolution and dynamics of already formed soliton structures. In 1984, Belashov [96] succeeded in analytical and numerical investigation of the evolution of solitons of the KdV equation on the non-stationary stage, i.e., he studied dynamics of the formation of solitons as (subsequently) stationary wave objects. The analytical study was based on a generalization of the IST method for the KdV equation considered in Sect. 1.2.3. The numerical studies were done on the basis of scheme (1.82) of numerical integration of the KdV equation. The results of these investigations demonstrated that:

1. The duration of the stage of the “non-stationary” evolution for every soliton of the solution  $u(t, x)$  is different and increases exponentially with the increasing “number” of the soliton (see Fig. 1.9).
2. The velocities of the solitons on the “non-stationary” stage decrease to their stationary values determined by the asymptotic expression

$$v_n(t, x) = \lim_{t \rightarrow \infty} \left[ \frac{u_n(t, x)}{3} \right],$$

where  $u_n$  is the amplitude of the  $n^{\text{th}}$  soliton (Fig. 1.10).

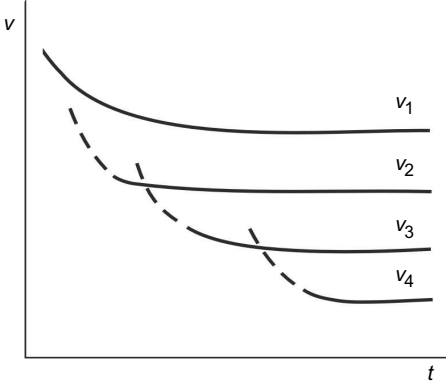


**Fig. 1.10.** Change of the soliton velocities on the stage of the “non-stationary” evolution

3. The growth dynamics of the soliton amplitudes also reveals the exponential character, with the exponent depending on the number of the soliton (Fig. 1.11).

It is interesting to note that the changes of the amplitudes and velocities (to their stationary asymptotic values) are inversely proportional to each other at this stage, while in the limit  $t \rightarrow \infty$  the amplitudes and velocities are directly proportional:

$$v_n = \frac{u_n}{3}.$$

We note again that all numerical results obtained for the “non-stationary” stage can be naturally interpreted within the limits of the (properly modified) IST theory.

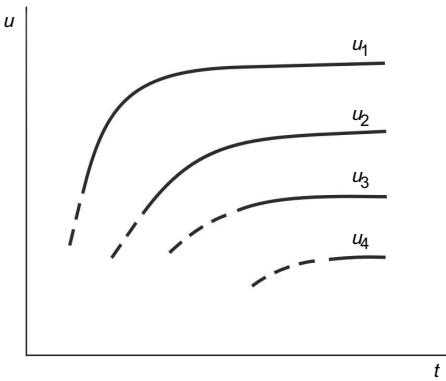


**Fig. 1.11.** Evolution of the soliton amplitudes on the stage of the “non-stationary” evolution

Consider now solutions of the KdV equation in the opposite limiting case when  $\sigma \ll \sigma_s$ . As demonstrated in Ref. [93], the “non-soliton” solutions corresponding to disturbances not decaying into solitons are observed in this

case. These solutions are fast-oscillating wave packets as shown in Fig. 1.12, looking qualitatively like the *self-similar solution* [3] (see below), although such a packet can differ quantitatively from the self-similar solution by the law with which the amplitude decreases in time and space. It is clear that

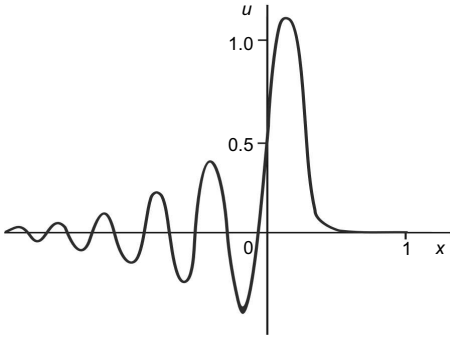


**Fig. 1.12.** Solution of the KdV equation with  $\sigma = 1.9$  ( $\beta > 0$ )

for  $\beta < 0$ , the picture is qualitatively opposite – a “train” of fast oscillations goes forward from the main maximum since with the change  $x \rightarrow -x$  we obtain the same KdV equation (1.11) but with  $\beta < 0$ . We also note that for some initial conditions, one can observe a solution of the clearly pronounced mixed type having (alongside with the solitons, propagating as the locally stationary objects) an oscillating “tail” falling behind from the solitons of the form similar to that shown in Fig. 1.12.<sup>8</sup>

Now, a few words about the *self-similar solution* of the KdV equation. If we consider a series of initial disturbances with  $l \rightarrow 0$  in (1.24) (see Sect. 1.1) but take into account that  $u_0 l^2 = \text{const}$ , then solutions for the same  $\beta$  appear to be similar since the parameter  $\sigma$  remains constant. Such a limit solution is given by [3]

$$u(t, x) = \frac{\beta}{(3\beta t)^{2/3}} \psi \left[ \frac{x}{(3\beta t)^{1/3}} \right]. \quad (1.102)$$

Substituting this solution into the KdV equation (1.11), limiting our study by the solutions  $\psi(z)$  exponentially decreasing at  $z \rightarrow \infty$ , and also assuming that  $\psi(z) = f'(z)$ , we obtain the Airy equation (for the function  $f(z)$ ),

$$f''(z) - zf(z) = 0.$$

Its solution for  $z \rightarrow \infty$  is the Airy function  $\text{Ai}(z)$  (1.32). Thus the asymptotics of the considered solutions for the function  $\psi(z)$  is given by [3]

<sup>8</sup> It is necessary, however, to state that, as was shown in Ref. [96] where evolution of the solitons on the “non-stationary” stage was studied in detail, in reality the non-soliton oscillating part of the solution is always present. The difference consists only in the comparative amplitudes of the solitons and the “tail.”



$$\psi(z) = c \frac{d\text{Ai}(z)}{dz} \approx -\frac{c}{2} z^{1/4} \exp\left(-\frac{2}{3} z^{3/2}\right) \quad \text{as } z \rightarrow +\infty.$$

Behavior of such solutions for not too large  $z > 0$  and  $z < 0$  was investi-

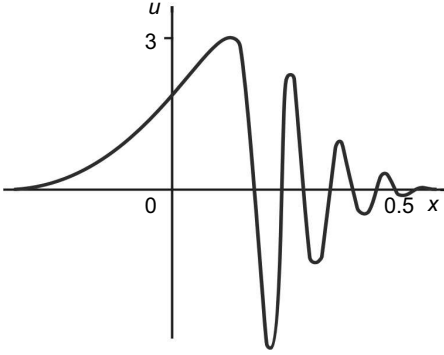


**Fig. 1.13.** Self-similar solution of the KdV equation with  $\beta < 0$  for  $\sigma = 10$  ( $z < 0$ )

gated numerically [93]. The studies showed (see Fig. 1.13) that the solution is qualitatively similar to the solutions of the linearized KdV equation (see Sect. 1.1) as well as the KdV equation with finite  $l$  in the initial condition and  $\sigma \ll \sigma_s$ . Physically, the self-similar solution (1.102) describes the evolution of initial disturbances given by

$$\partial_x \left[ \left( \frac{C}{\pi^{1/2}} \right) \exp(-x^2/l^2) \right]$$

for  $x \gg l$  and  $t^{1/3} \gg l/\beta^{1/3}$ , where  $C = u_0 l^2 = \text{const}$ , i.e.,  $u_0 = C/l^2$  is the characteristic velocity.

Consider now the character of the solution of the KdV equation with the initial condition taken as a “smoothed step,”

$$u(0, x) = \frac{c}{1 + \exp(x/l)}, \quad (1.103)$$

where  $l$  gives the width of the front of the initial disturbance. As a result, the step (1.103) evolves into the wave “train” (Fig. 1.14). The amplitude of the first oscillation achieves its stationary value proportional to  $c$ . This result was obtained in Ref. [93] by employing the implicit scheme represented by (1.84).

We see that various initial disturbances lead, within the limits of the KdV model, to different sorts of solutions. The form of a particular solution is defined (for the same initial condition) by the dispersion parameter  $\beta$  (or  $\sigma$  in the KdV equation (1.26)). Thus we demonstrated in the above examples that numerical methods presented here can be effectively used for numerical

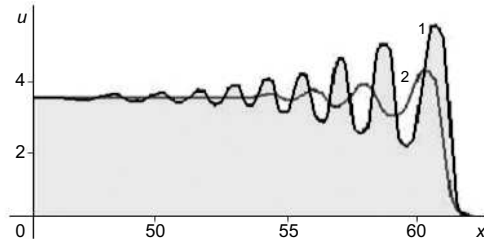


**Fig. 1.14.** Solution of the KdV equation for the initial condition (1.103) with  $c = 4$  at  $t = 0.9$ . Curve 1 – without dissipation, curve 2 – with dissipation, see (2.2) in Sect. 2.1

integration of the KdV-class equations. More KdV-class equations generalizing the KdV model and taking into account the dissipation, instability, and higher order dispersion correction are considered below in specially dedicated sections of Chap. 2.

## 1.4 Ion-Acoustic Waves in Plasmas

In this section we consider applications of the results obtained for the KdV equation in the previous sections to description of the structure and dynamics of one-dimensional waves in a plasma. We consider ion-acoustic waves in an unmagnetized plasma and we also include discussions on weakly-relativistic effects.

### 1.4.1 The Ion-Acoustic Waves

In the Introduction section, we already mentioned that both the KdV-class and KP-class equations are universal in the sense that they describe a wide class of nonlinear wave motions in dispersive media. In Sect. 1.1 we demonstrated the above for the KdV equation (1.11) when the dispersion law in the linear approximation can be written as

$$\omega = c_0 k \left( 1 - \frac{\beta k^2}{c_0} \right), \quad (1.104)$$

where  $c_0$  is the phase velocity of the wave and the factor  $\beta$  is determined by the particular type of the medium considered. In this section, we consider one of numerous applications of the KdV-class equations and study *ion-acoustic waves* in an unmagnetized plasma, when the dispersion parameter and the phase velocity are given by

$$\beta = c_0 r_D^2 / 2 \quad \text{and} \quad c_0 = c_s = (T/m_i)^{1/2}. \quad (1.105)$$

Here,  $r_D = (T_e / 4\pi n_e e^2)^{1/2}$  is the electron Debye length,  $T_e$  is the electron temperature (in energy units such that the Boltzmann constant is unity),  $n_e$

is the unperturbed electron density,  $c_s$  is the speed of the ion sound,  $T$  is the effective temperature (e.g., equal to  $T_e$  when  $T_i \ll T_e$ ), and  $m_i$  is the ion mass.

The ion-acoustic wave is a mode commonly occurring in both collisionless and collisional plasmas. Physically, in a collisionless and non-isothermal plasma where the electron temperature is much larger than the ion temperature ( $T_e \gg T_i$ ), these waves are driven by the electron pressure and ion inertia, the coupling between the species being achieved by the electrostatic forces. Although the dispersion relation remains similar to that of the collisionless case, the physics of the ion-acoustic waves in a *collision-dominated plasma* is more complicated, since both electrostatic and collisional effects enter into play [99]. For example, collisions between the dissimilar particles can also couple the dynamics of the ions and the electrons. Thus, the collisional ion-acoustic waves can involve both plasma and neutral-fluid properties. Furthermore, collision-driven resistive and dissipative instabilities can occur if external free-energy sources, such as external currents, density and velocity inhomogeneities, etc., are present [100–103], and the waves can become nonlinear and/or turbulent.

### 1.4.2 Nonrelativistic Approximation

Assume that a plasma has two fully ionized components (electron and ion) and can be approximated by two-fluid hydrodynamics when the electron and ion components are described by the equation of motion and the continuity equations of type (1.1):

$$\begin{aligned}\partial_t \mathbf{v}_{e,i} + (\mathbf{v}_{e,i} \cdot \nabla) \mathbf{v}_{e,i} &= -(nm_{e,i})^{-1} \nabla p_{e,i} - (e_{e,i}/m_{e,i}) \nabla \varphi, \\ \partial_t n_{e,i} + \nabla \cdot (n_{e,i} \mathbf{v}_{e,i}) &= 0.\end{aligned}\tag{1.106}$$

In addition, instead of the Laplace's equation (1.3), we have the Poisson's equation for the electric potential  $\varphi$ :

$$\Delta \varphi = -4\pi e(n_i - n_e).\tag{1.107}$$

In these equations, the subscripts  $e, i$  stand for the particle type (electron or ion, respectively) and for simplicity we assume that  $-e_e = e_i \equiv e$ . Furthermore, we suppose that the plasma is non-isothermal, i.e., its (electron and ion) components have distinctively different temperatures,  $T_i \ll T_e$  (and, correspondingly, the different pressures,  $p_{e,i} \sim n_{e,i} T_{e,i}$ ), and consider the low-frequency branch of the oscillations when the condition

$$\tau^{-1} \ll \omega_{pe} = (4\pi n_e e^2 / m_e)^{1/2}$$

is satisfied. Assume also that the electrons are Boltzmann-distributed, i.e., their relaxation time is very short compared to the period of the ion plasma

oscillations [3]. In the limit  $T_i \ll T_e$  the low-frequency oscillations are weakly damped, and one can further assume that  $T_i = 0$  (and therefore in the following section,  $T$  can stand for the electron temperature  $T_e$ ).

Thus omitting the index  $i$  for the ion velocities and number densities, we can rewrite Eqs. (1.106) and (1.107) as

$$\begin{aligned}\partial_t \mathbf{v} + (\mathbf{v} \cdot \nabla) \mathbf{v} &= -(e/m_i) \nabla \varphi, \\ \partial_t n + \nabla \cdot (n \mathbf{v}) &= 0, \\ \Delta \varphi &= 4\pi e [n_0 \exp(e\varphi/T) - n].\end{aligned}\tag{1.108}$$

For the long wavelength *ion-acoustic waves* when  $kr_D \ll 1$  (the condition of weak dispersion), the dispersion relation (1.12) is valid. Now, using the technique used above in Sect. 1.1 to derive the KdV equation, we can easily obtain the *Boussinesq equations* for the ion-acoustic wave,

$$\begin{aligned}\partial_t \mathbf{v} + (\mathbf{v} \cdot \nabla) \mathbf{v} &= -c_s^2 \nabla \ln n - (2c_s \beta / n_0) \nabla \Delta n, \\ \partial_t n + \nabla \cdot (n \mathbf{v}) &= 0\end{aligned}\tag{1.109}$$

(compare with (1.7) in Sect. 1.1), where  $\beta$  and  $c_s$  are defined by (1.105).

Consider the wave propagating along the  $x$ -axis when the  $x$ -component of the ion velocity is much smaller than the phase velocity  $c_s$ . In this case, following the results of Sect. 1.1, we obtain the KdV equation for propagation of the ion-acoustic wave in the  $x$ -direction:

$$\partial_t v + c_s \partial_x v - c_s \delta^2 \partial_x^3 v + v \partial_x v = 0,\tag{1.110}$$

where  $\delta^2 = r_D^2/2 = \beta/c_s$ , which is similar to (1.10). After the homothetic transformation and transition to the reference frame moving along the  $x$ -axis with the velocity  $c_s$ , we obtain the *KdV equation* in its standard form

$$\partial_t u + \alpha u \partial_x u + \beta \partial_x^3 u = 0,\tag{1.111}$$

where  $u$  is the velocity of the ion “sound,” and the factor at the nonlinear term is  $\alpha = 3c_s/2n$  [3].

Turning to (1.110), we note that the term  $c_s \partial_x v$  describes the wave propagating in the  $x$ -direction with the velocity  $c_s$ , while the dispersion and nonlinear terms are responsible for slow changes of the sound wave field on the background of the fast wave motion with the velocity  $c_s$ . Such type of sound waves is mostly characteristic of isotropic media (e.g., plasma without magnetic field), but sometimes it takes place in an anisotropic medium as well. For example, if the characteristic frequencies of the ion-acoustic wave packet are much larger than the ion-cyclotron frequency,  $\omega_{Bi} = eB_0/m_i c$ , appearing in a magnetized plasma, the plasma anisotropy can be neglected and one can still reduce (1.110) to the KdV equation (1.111). In the opposite case, when

$\omega \ll \omega_{Bi}$ , the effects of the anisotropy cannot be neglected and it is necessary to consider a non-one-dimensional model<sup>9</sup> (see, for example, Sect. 4.6).

Finally, we note that it is not necessary to specially integrate (1.111), since all results of the previous sections can be applied directly to this case of the ion-acoustic waves in a collisionless unmagnetized plasma. What is necessary is merely to interpret them properly, taking into account the physics behind the terms and factors of this equation.

### 1.4.3 Weakly-Relativistic Effects

As we demonstrated above, ion-acoustic waves in a plasma can be described by the KdV equation (1.111). If velocities of plasma particles approach the speed of light, the relativistic effects should be taken into account when considering propagation of the one-dimensional solitary ion-acoustic wave. It appears that the *relativistic effects* can strongly influence the phase velocity, the amplitude, and the characteristic length of the wave.

Using the reduced perturbation method [104] for the one-dimensional ion-acoustic solitary waves in a weakly relativistic collisional plasma, we can obtain the KdV equation of type (1.111) by taking into account the relativistic factor  $u/c$ :

$$\partial_\tau \Phi_1 + \alpha(\vartheta_1) \Phi_1 \partial_\xi \Phi_1 + \frac{1}{2} \beta(\vartheta_1) \partial_\xi^3 \Phi_1 = 0, \quad (1.112)$$

where  $\Phi_1 = \vartheta_1^{1/2} u_1$  is the first-order perturbation of the electrostatic potential  $\Phi = \varepsilon \Phi_1 + \varepsilon^2 \Phi_2 + \dots$  ( $\varepsilon$  is the small expansion parameter),  $u_1$  is the first-order perturbation of the particle velocity ( $u = u_0 + \varepsilon u_1 + \varepsilon^2 u_2 + \dots$ ), and

$$\begin{aligned} \alpha(\vartheta_1) &= \beta(\vartheta_1) \left( 1 - \vartheta_2 / \vartheta_1^{3/2} \right), & \beta(\vartheta_1) &= \vartheta_1^{-1/2}, \\ \vartheta_1 &= 1 + 3u_0^2 / 2c^2, & \vartheta_2 &= 3u_0 / 2c^2. \end{aligned} \quad (1.113)$$

Equation (1.112) is written for the reference frame moving along the  $x$ -axis,  $\xi = \varepsilon^{1/2}(x - \lambda t)$  and  $\tau = \varepsilon^{3/2}t$ , where  $\lambda$  is the phase velocity. Note that the factor at the nonlinear term is positive,  $\alpha > 0$ , because of  $\vartheta_1 \gg \vartheta_2$ . In this case we can obtain a stationary solution in the form of a solitary wave. Introducing a new variable  $\zeta = k\xi - \omega\tau$  and substituting it into (1.112), we write the solution for the one-dimensional wave in the form of the *ion-acoustic soliton*:

$$\Phi_1 = \Phi_0 \cosh^{-2} \left( \frac{\zeta}{kW} \right). \quad (1.114)$$

Here, the amplitude  $\Phi_0$  and the characteristic scale  $W$  are given by

<sup>9</sup> On the right-hand side of the equation of motion (1.107), an additional term proportional to  $\omega_{Bi} \hat{\mathbf{x}} \times \mathbf{v}$  (where  $\hat{\mathbf{x}}$  is the unit vector of the  $x$ -axis) appears and it is necessary to include an additional term that is proportional to  $k_\perp^2 / 2k_x^2$  into dispersion relation (1.104) (see also comment in Sect. 4.6.1).

$$\Phi_0 = \frac{3\delta}{\alpha(\vartheta_1)} \quad \text{and} \quad W = \left[ \frac{2\beta(\vartheta_1)}{\delta} \right]^{1/2}, \quad (1.115)$$

where  $\delta = \omega/k$  and the boundary conditions are  $\Phi_1 \rightarrow 0$ ,  $\partial_\zeta^n \Phi_1 \rightarrow 0$  for  $n = 1, 2$  and  $|\zeta| \rightarrow \infty$ . The dispersion law for the described waves has the form  $\omega = 2\beta(\vartheta_1)k^3$ .

**Table 1.2.** Comparison of results (1.113)–(1.115) with those of Refs. [105,106]

Parameter	Eqs. (1.113)–(1.115)	$u_0/c = 0$ [105,106]	$u_0/c \neq 0$ [105,106]
$\lambda$	$u_0 + \vartheta_1^{-1/2}$	1	$u_0 + \vartheta_1^{-1/2}$
$\alpha$	$(1 - \vartheta_2/\vartheta_1^{3/2})/\vartheta_1^{1/2}$	1	$(1 - \vartheta_2/\vartheta_1^{3/2})/\vartheta_1^{1/2}$
$\beta$	$\vartheta_1^{-1/2}$	1	$\vartheta_1^{-1/2}$
$\Phi_0$	$3\delta\vartheta_1^{1/2}/(1 - \vartheta_2/\vartheta_1^{3/2})$	$3s$	$3s\vartheta_1^{1/2}/(1 - \vartheta_2/\vartheta_1^{3/2})$
$W$	$\vartheta_1^{-1/4}(2/\delta)^{1/2}$	$(2/s)^{1/2}$	$\vartheta_1^{-1/4}(2/s)^{1/2}$

We can see from (1.113) that factors at the nonlinear term as well as at the dispersion term are determined by the relativistic factor  $\vartheta_1$ , and relations (1.115) show the dependence of the amplitude and the characteristic scale of the KdV ion-acoustic soliton on the (weakly) relativistic effects. Comparison of results following from (1.113)–(1.115) with those for the two extreme cases  $u_0/c = 0$  and  $u_0/c \neq 0$  considered in Refs. [105,106] is given in Table 1.2. Here,

$$s = \omega/k \cong v_0 + \vartheta_1^{-1/2} (1 - k^2/2),$$

where  $v_0$  is the ion velocity (if  $v_0 \sim 0$  and the relativistic effects are absent then  $s \cong 1 - k^2/2$ ). We see from Table 1.2 that the results obtained above also include the cases considered in Refs. [105,106].

Consideration of effects in a weakly-collisional and weakly-relativistic plasma is justified by a number of phenomena in a plasma where high energy flows of a particles should be taken into account. In particular, when the kinetic energy of ions,  $Mu_0^2/2$ , reaches 4.7MeV for  $u_0/c \approx 0.1$ , a weakly-relativistic ion-acoustic solitary wave starts to form, thus describing the motion of high energy protons with the velocity approaching the speed of light, as observed in the Earth's *magnetospheric plasma* [107]. Investigation of the relativistic nonlinear waves also has application in laser plasma physics [108] and astrophysics [109].

Solitary Waves in Dispersive Complex Media

Theory, Simulation, Applications

Belashov, V.Y.; Vladimirov, S.V.

2005, XIV, 294 p., Hardcover

ISBN: 978-3-540-23376-3